4. PIXE AND LA-ICP-MS CONSTRAINTS ON ORE FLUID COMPOSITIONS AT THE OSBORNE IOCG DEPOSIT, MOUNT ISA INLIER, AUSTRALIA

4.1 Introduction

In the previous chapters the fluid inclusion populations in the Osborne silica flooding and pegmatite samples have been classified and the sources of the fluids and their salinity investigated. In this chapter PIXE (proton induced X-ray emission) and LA-ICP-MS (laser ablation inductively coupled plasma mass spectrometry) are used to further investigate ore depositional processes, the composition of the ore-forming fluids and their sources. Selected fluid inclusions have been analysed by both methods, enabling direct comparison of two microanalytical techniques. Both PIXE and LA-ICP-MS, which permit the analysis of individual fluid inclusions, are becoming increasingly widely used in studies of hydrothermal ore deposits (Ulrich et al., 1999; Ryan et al., 2001; Williams et al., 2001; Heinrich et al., 2003; Baker et al., 2004; Mustard et al., 2006; Williams et al., in press). However, there is very limited data on how the two techniques compare when used on the same samples.

4.2 Methods

4.2.1 PIXE

Selected aqueous brine inclusions and CO_2-bearing brine inclusions (MS- and CB-type; see Chapter 2) were studied by non-destructive proton induced X-ray emission (PIXE) analysis, using the CSIRO-GEMOC Nuclear Microprobe at CSIRO, North Ryde, Sydney. Inclusions in each sample have been characterised by microthermometry, however due to the observed tendency of high salinity fluid inclusions at Osborne to

decrepitate prior to homogenization the individual inclusions chosen for PIXE analysis were not subjected to microthermometric examination. The initial study was conducted on a limited number of samples in 2002 with further samples analysed in 2003. The samples were collected by Roger Mustard who identified inclusions for analysis and carried out the analysis. The raw data were reduced, refitted and analytical artifacts removed in this study allowing the analyses to be interpreted.

A microfocused beam of 3 MeV was used with experimental conditions largely as described by Ryan et al. (1991) but utilizing beam-scanning techniques that create a uniform beam dose distribution leading to significantly-improved reproducibility and quantification (Ryan et al., 1995). The compositions of MS and CB inclusions were quantified using the model of Ryan et al., (1993) in which the element of interest is situated at a discrete point (x,y,z) within a fluid inclusion buried in a sample matrix. The parameters required for these calculations are the densities of the matrix and the fluid, their proton-stopping powers, the X-ray production cross sections, the X-ray absorption coefficients, and the detector sensitivity for each element (e.g. Kurusawa et al., 2003).

The Osborne fluids were modelled as H_2O and their density was corrected using microthermometric estimates of the salinity. In the absence of a large vapour bubble MS inclusion densities were given based on an homogenised brine, typically 1.1 g/cc (similar to those calculated from microthermometric data, see Chapter 2), while for CB inclusions which contain a significant low density carbonic phase densities were estimated at 0.8 g/cc. The inclusion sizes and depths were determined with an optical microscope, based upon focusing positions. In some cases inclusion depths can be verified through PIXE analysis by examination of Cl K X-rays. Cl K X-rays are

strongly absorbed by silica in the quartz mineral host which makes Cl most sensitive to inclusion depth and in high salinity inclusions the absorption can affect the relative intensity of Cl K_α and K_β X-rays so that examination of the differential absorption of Cl K_α and K_β X-rays can provide a direct measure of inclusion depth in shallow inclusions (Ryan et al., 1995). In inclusions where NaCl concentrations exceed 10wt% an examination of the least-squares fit to the PIXE inclusion spectrum using yields corresponding to a range of depths can be used to determine the inclusion depth to within 1.5μm (Ryan et al., 1993; Ryan et al., 1995).

In earlier studies a quantitative measure of the composition of individual synthetic euhedral fluid inclusions was achieved with an accuracy of ~10-15% for inclusions containing small vapour bubbles and no daughter crystals (Ryan et al., 1995). Modelling has suggested this accuracy could be increased to 30% for light elements such as Cl in analyses of inclusions containing solid phases though elements with high atomic masses are far less sensitive to internal structure of a fluid inclusion. The typical suite of elements detected in the Osborne inclusions includes Cl, K, Ca, Mn, Fe, Cu, Zn, As, Br and Pb, with Ti, Ge, Rb, Sr, Ba and Bi occurring in concentrations above the detection limits in some cases. Mo, Ag, Sn, Sb and Cs were also analysed but are below detection limits in all inclusions. S may be detected but cannot be properly quantified.

Analyses of natural fluid inclusions will have greater errors due to uncertainties in estimation of inclusion depths and thickness, and deviations from the model ellipsoidal geometry. These geometry-related errors will vary and may exceed 20%. However, inter-element ratios, particularly for elements with similar atomic numbers,

will be more accurate than estimates of actual concentrations because the main sources of error will impact on all element analyses to a similar degree. On figures showing PIXE data in this chapter error bars are marked at 30% error for all elements, except Cl which has errors of up to 50%. Analysis is typically considered to be effective only in inclusions at depths of less than 20 microns below the sample surface (Ryan et al., 1993).

The inclusions were imaged as X-ray maps providing information on distribution of elements within phases (e.g. Williams et al., 2001; Fig 4.1). An important advantage of the imaging PIXE technique of Ryan et al., (2001) is the ability to identify and exclude nearby solid inclusions in quartz that could otherwise contaminate the analysis. These images do not remove artifacts created by X-ray 'pile-ups' or elevated background created by some phases (e.g. Fe-rich solids). The addition of X-ray peaks from Fe and Si results in an artificial interference with the Cu peak, producing a signal equivalent to >100ppm Cu in some Fe-rich inclusions. The 'pile-up' of X-rays creates a 'wedge' on the spectra which obscures the Cu peak and contributes artificially to the Cu signal (Figure 4.2). Examination of the shape of the Cu peak on the spectra for each inclusion allows this effect to be identified and removed and actual Cu peaks to be recognised and Cu concentrations to be determined where possible. For almost all inclusions the subtraction of the pile-up effect lowers the measured Cu concentration to below detection limits. In this study the detection limit for Cu was typically between 20 and 60ppm dependent on fluid inclusion geometry. An artificially elevated As signal was also identified in some samples, with the X-ray spectra fit over-estimating the peak volume (Fig. 4.3A). There are both As and Pb X-ray contributions to this peak with As

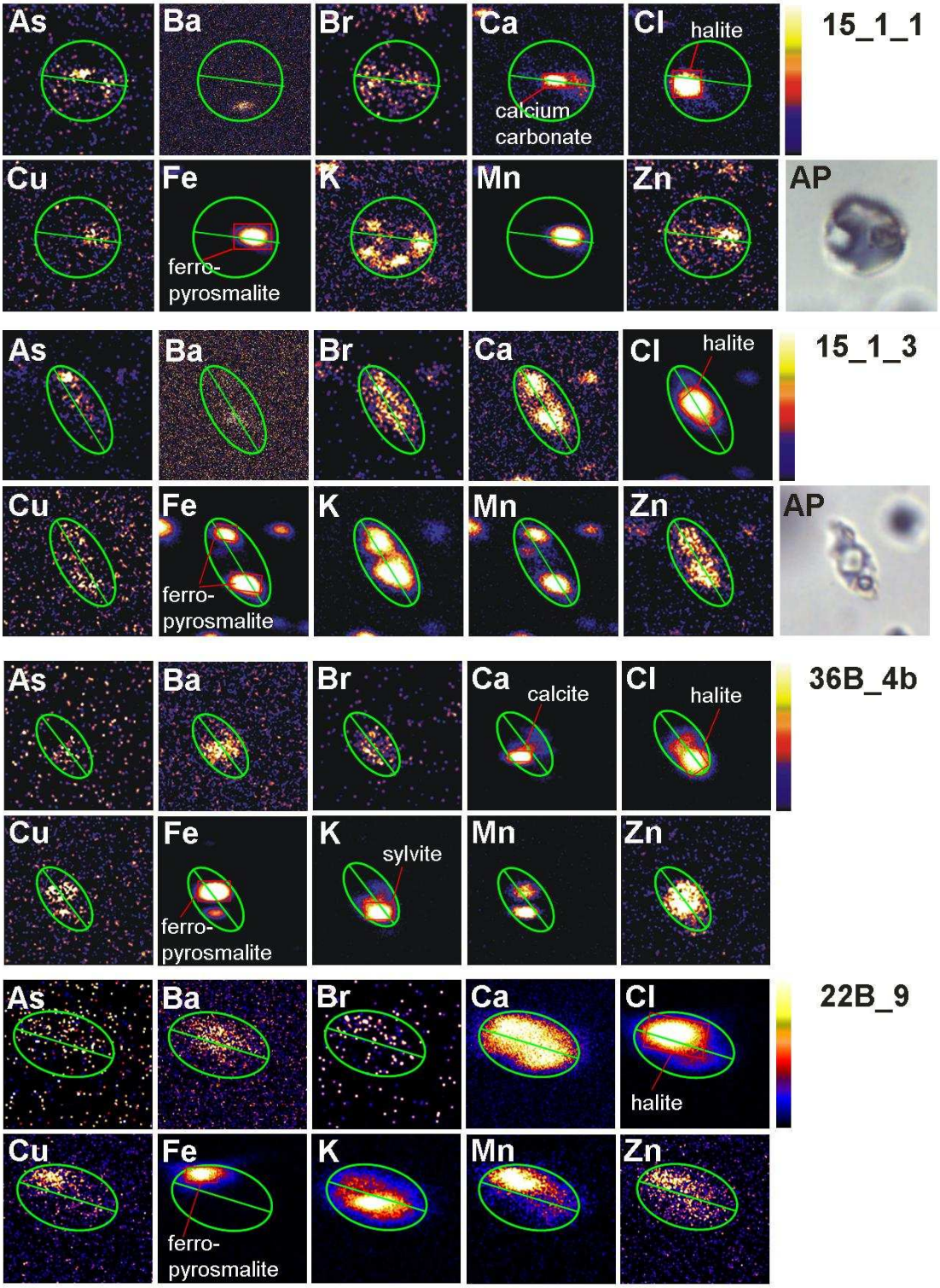

Figure 4.1: Representative PIXE element maps showing CB and MS type inclusions from three samples at Osborne.
(15_1_1) a CO_2-bearing brine (CB) inclusion from sample Osb15; (15_1_3) a multi-solid brine (MS) inclusion. K, Ca and Zn can be seen to vary in association, being observed associated with solid phases and dissolved with the liquid phase. Ca is part of a carbonate solid in the CB type inclusion while remains dissolved in MS inclusions. Cu shows an association with an Fe- and Mn- bearing phase but this has been shown to be an product of Fe-Silica pile-up; (22B_9) Ca and Ba are dissolved in the fluid phase; (36B_4b) Ca and Ba show an association with a solid phase. A full set of images for each inclusion analysed is given in Appendix H.

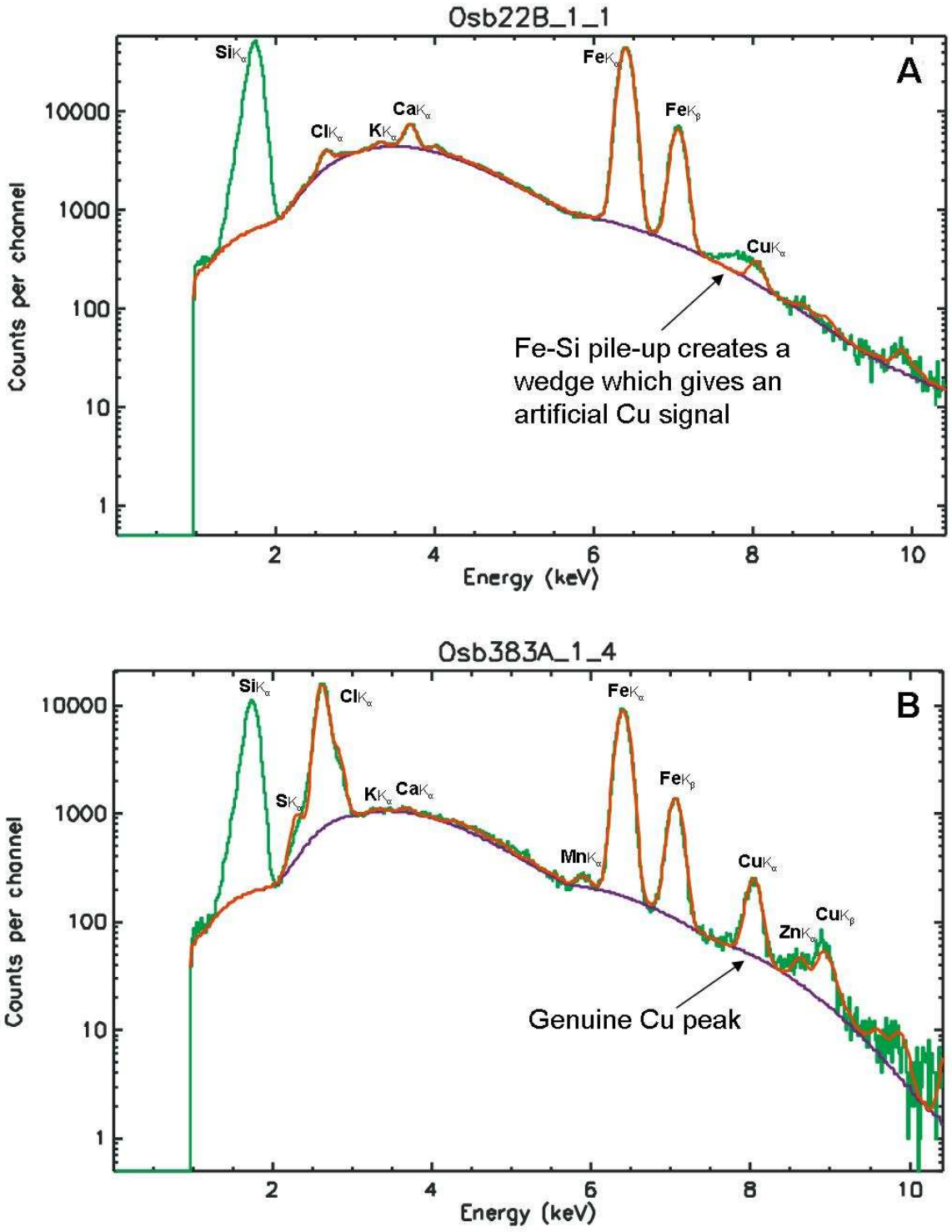

Figure 4.2: X-ray spectra for two MS inclusions at Osborne showing true and artificial Cu peaks..

(A) Osb22B_1_1 shows a wedge shaped iron-silica pile-up feature which gives an artificial Cu signal.

(B) Osb383A_1_4 shows a genuine Cu peak (sample not part of this study due to uncertainties regarding location).

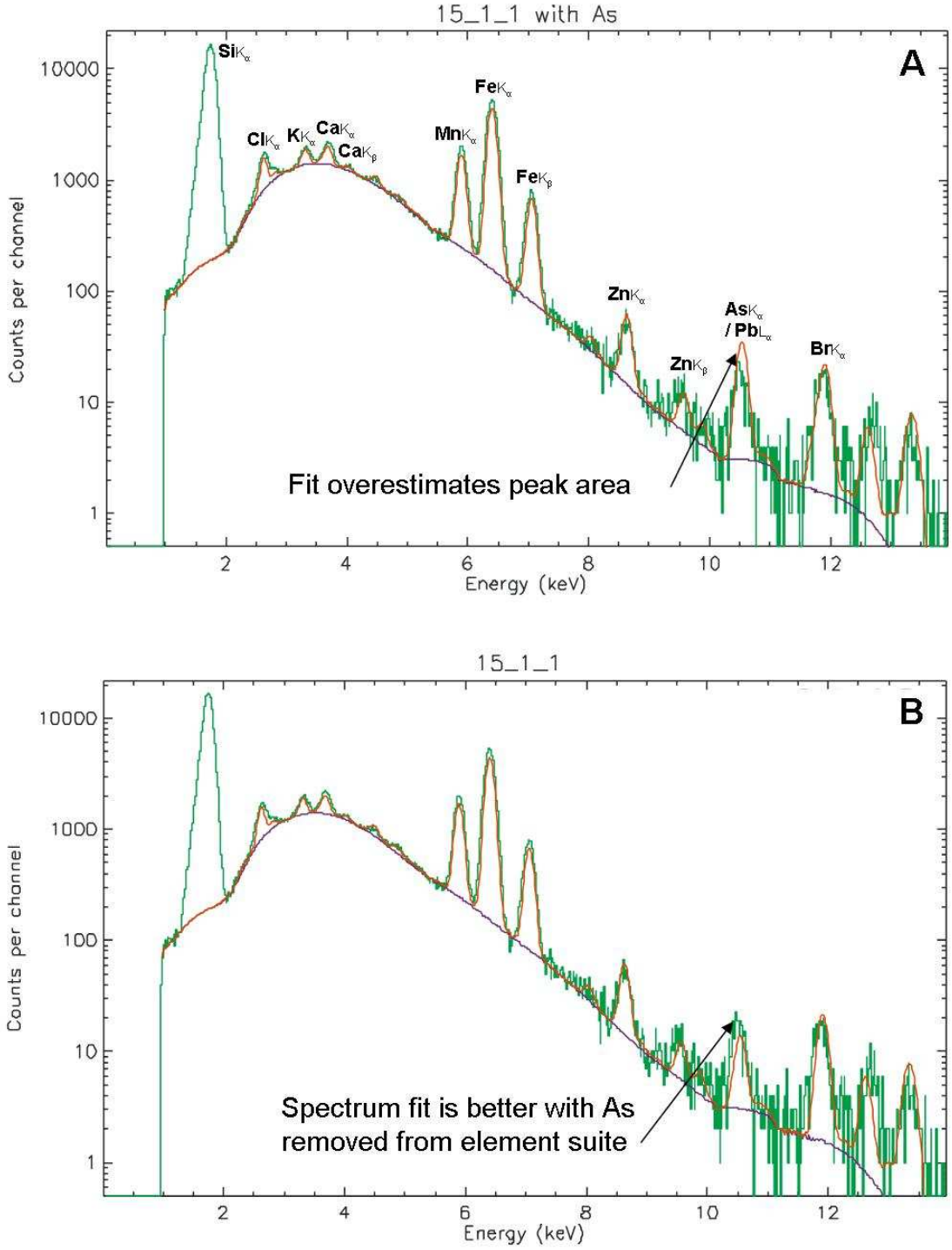

Figure 4.3: X-ray spectra fit for inclusion 15_1_1 with and without As included in fit.

(A) With As included in the fit the peak volume is overestimated. As contribution to the peak is less than Pb contribution, resulting in overestimation of As concentrations.

(B) With As removed from the element suite, the fit to the peak is better, suggesting the majority of the peak is attributable to Pb X-rays (see text).

K_α at 10.506 keV and Pb L_α at 10.448 keV. When As is removed from the fit the peak fit is better (Fig. 4.3B), suggesting that the As contribution is negligible.

4.2.2 LA-ICP-MS

Fluid inclusion bearing samples from the Osborne deposit were studied and high and moderate salinity brine and CO_2-bearing brine inclusions (MS, LVD and CB-type, see chapter 2) were identified for further analysis by Roger Mustard. Individual fluid inclusions were analysed by laser ablation inductively coupled mass spectrometry (LA-ICP-MS), a powerful and efficient multi-element microanalytical technique. The analysis was conducted using a 193nm ArF Excimer laser combined with an Agilent 7500s ICP-MS located at the Research School of Earth Sciences at the Australian National University. The data were normalised to salinities determined by microthermometry in this project (Chapter 2) allowing the analyses to be interpreted. A limited number of inclusions ablated had previously been analysed by PIXE (see sections 4.2.1; 4.3).

Forty-two inclusions from four samples (from the 1S and 3E ore lense and a pegmatite) were selected for analysis, with complete data collected for 31 inclusions, mainly MS and CB (Appendix F). The laser spot size was adjusted to the size of the inclusion and ablation continued until the entire inclusion was sampled and the laser drilled the underlying host mineral. The integrated intensities (counts/second) of the fluid inclusion signals from each analysis were background corrected and further corrected for matrix contributions as even quartz, which is compositionally simple, may contain trace elements at high concentrations (Dennen, 1964; 1966; Flem et al., 2002; Müller et al., 2003; Götze et al., 2004). The duration of peaks for all elements were compared

with the duration of the Na peak, allowing matrix additions to be removed and analyses in which the halite solids were inefficiently ablated to be identified. Analytical errors and matrix effects can be minimised since only well-ablated inclusions were chosen for the calculation and all signals are scanned for spikes.

Instrument drift was linearly corrected by application of the bracketing method of an external standard (NIST 612). The concentrations, detection limits (3σ) and sensitivities were calculated for each inclusion individually using the method of Longerich et al., (1996). The equivalent wt% NaCl value from microthermometric experiments on inclusions of the same type in each sample was used as an internal standard. Average salinities for MS inclusions from each sample were used, typically between 45-60 wt% NaCl equivalent (see section 2.4.3). The use of average salinities will increase the error in the analyses, with a 5% error in the estimated salinity resulting in estimated 10-20% errors in the data.

Elements routinely detected	Elements frequently detected	Elements rarely/never detected
^{3}Na	^{24}Mg	^{118}Sn
^{39}K	^{47}Ti	^{140}Ce
^{43}Ca	^{59}Co	^{197}Au
^{55}Mn	^{65}Cu	^{209}Bi
^{57}Fe	^{121}Sb	
^{58}Ni	^{133}Cs	
^{64}Zn		
^{66}Zn		
^{75}As		
^{85}Rb		
^{88}Sr		
^{138}Ba		
^{208}Pb		

Table 4.1: Suite of elements analysed for by LA-ICP-MS
Concentrations for all elements with more than one stable isotope are calculated from natural isotope ratios. Where mass-interferences cause problems with analysis, lower abundance isotopes are measured (e.g. ^{43}Ca) and true concentrations calculated from natural isotope ratios – a process that introduce larger errors.

The suite of elements typically detected by this method include Na, K, Ca, Mn, Fe, Ni, Zn, As, Rb, Sr, Ba and Pb (Table 4.1). Na is of particular interest as it is not detected by PIXE analysis. Other elements, detected in some inclusions analysed include Mg, Ti, Co, Cu, Sn, Sb, Ce, Cs and Bi. Au was analysed for but not detected except in one sample where an Fe-solid (probably pyrite) external to the fluid inclusion was also believed to have been unintentionally analysed.

4.3 Fluid Inclusion Geochemistry Results

PIXE analyses focused on primary MS and CB inclusions (hosted by silica-flooding quartz) which can be considered to have entrapped high salinity pre-depositional ore fluids. LA-ICP-MS analyses also focused on CB and MS inclusions, however a limited number of secondary LVD inclusions, considered to be representative of 'spent' post-deposition ore fluids, were also analysed. The full data sets for each method can be found in Appendices E and F.

Major cation concentrations measured for each inclusion by both methods are given in tables 4.2 and 4.3 and element ratios are given in tables 4.4 and 4.5. A limited number of inclusions in each sample were analysed by both methods, providing a direct comparison (Table 4.6). As the average concentrations of major cations measured by the two methods vary by up to an order of magnitude it is more effective to compare the elemental ratios (Fig. 4.4). Also the main causes of errors for each method produce similar effects for all element analyses so elemental ratios should be relatively accurate. In six of the ten inclusions analysed by both methods the Mn/Fe values are within 10% error of one another. K/Fe values show greater variation with the few values being

Sample	PIXE Element Concentration Range										
	(Wt %)			(ppm)							
	Cl	Fe	Mn	K	Ca	Cu	Zn	Pb	Br	As	Ba
15 (1S)	2.8 – 44.0	2.3 – 9.8	0.62 – 2.6	4080 – 28390	3280 – 29160	<200	460 – 2250	300 – 1570	280 – 4140	550 – 3940	910 – 4410
22B (1S)	0.3 – 68.3	<0.1 – 9.0	<0.1 – 0.6	2010 – 35350	3600 – 31710	<430	<25 – 990	<50 – 530	65 – 360	<20 – 840	<410 – 3280
36B (2M)	2.0 – 51.0	5.6 – 21.7	0.22 – 1.3	480 – 84460	420 – 38960	< 570	<120 – 1070	175 – 1760	70 – 1010	45 – 740	630 – 3080
37B (3E)	1.3 –54.7	1.3 – 20.7	0.07 – 1.4	7510 – 71030	910 – 25990	< 290	140 – 2880	170 – 2470	100 – 570	170 – 1010	670 – 4510
315 (1S)	<0.1 – 71.9	<0.1 – 9.4	<0.1 – 1.7	200 – 93210	370 – 38920	<540	20 – 2300	<550	<50 – 840	<25 – 300	90 – 6130
852 (Peg)	0.4 – 10.2	1.2 – 7.6	0.22 – 1.6	3780 – 88900	1650 – 25300	< 190	380 – 2490	230 – 1630	<40 – 180	400 – 1330	<280 – 1560

Table 4.2: Concentration ranges of selected major and trace elements measured by PIXE in MS and CB inclusions. Analysis of all elements incur errors of ±30%, excepyt for Cl which has analytical errors of ±50%. Full data set in Appendix E

Sample	LA-ICP-MS Element Concentration Range									
	(Wt %)			(ppm)						
	Na	Fe	Mn	K	Ca	Cu	Zn	Pb	As	Ba
15 (1S)	3.4 – 21.6	0.3 – 10.8	0.5 – 12.6	4740 – 177460	8620 – 243590	30 – 925	720 – 11270	80 – 7610	50 – 2850	700 – 14625
37B (3E)	7.6 – 11.0	8.7 – 17.2	0.5 – 10.6	30540 – 55340	12460 – 59490	15 – 50	850 – 3315	130 – 1080	20 – 520	1270 – 7230
852 (Peg)	3.4 – 10.7	0.5 – 6.6	0.02 – 0.05	25740 – 54090	20960 – 28510	7 – 13	1530 – 33130	60 – 3390	18 – 260	1390 – 4140

Table 4.3: Concentration ranges of selected major and trace elements measured by LA-ICP-MS in CB, MS and LVD inclusions. Full data set in Appendix F

		K/Ca	Fe/Ca	K/Mn	Mn/Fe	K/Fe	Br/Cl	Zn/Pb
1S	**Min**	0.81	3.37	0.4	0.09	0.11	0.28	0.97
	Max	6.3	8.3	3.62	0.31	1.02	16.49	8.87
	Avg	2.86	5.96	2.16	0.25	0.48	5.74	3.44
2M	**Min**	0.28	2.38	0.03	0.04	0.002	0.17	1.09
	Max	5.18	126.6	10.56	0.13	0.91	1.7	455.84
	Avg	2.85	30.03	6.12	0.08	0.51	0.8	92.52
3E	**Min**	2.18	4.03	2.94	0.05	0.2	0.63	1.67
	Max	8.62	14.37	9.82	0.07	0.6	0.91	4.92
	Avg	4.27	10.25	6.97	0.06	0.43	0.45	2.62
PEG	**Min**	2.15	1.49	1.26	0.06	0.29	0.14	0.24
	Max	6.18	7.69	40.22	0.24	4.13	0.44	3.35
	Avg	3.77	4.79	13.8	0.15	1.44	0.19	1.63

Table 4.4: Selected element ratios measured by PIXE in CB and MS inclusions.
Values are derived from analyses above detection limit. Where elements are not detected lower minimum and higher maximum ratios may be implied.

		Na/K	Na/Ca	K/Ca	Fe/Ca	Mn/Fe	K/Fe	Zn/Pb
1S	**Min**	0.13	0.18	0.15	0.03	0.05	0.08	0.43
	Max	26.6	20.6	3.69	11.61	6.75	29.08	68.79
	Avg	5.72	4.45	1.28	2.13	0.75	2.24	7.58
3E	**Min**	1.65	1.3	0.79	1.85	0.03	0.21	1.46
	Max	3.08	8.86	3.09	12.24	0.1	0.63	6.23
	Avg	2.14	4.07	1.85	5.3	0.06	0.4	3.13
PEG	**Min**	1.34	1.64	1.23	0.26	0.04	0.45	0.77
	Max	3.77	5.1	2.32	2.98	0.14	4.74	289.85
	Avg	2.2	3.41	1.63	1.86	0.09	2.06	99.47

Table 4.5: Selected element ratios measured by LA-ICP-MS in CB, MS and LVD inclusions.
Values are derived from analyses above detection limit. Where elements are not detected lower minimum and higher maximum ratios may be implied.

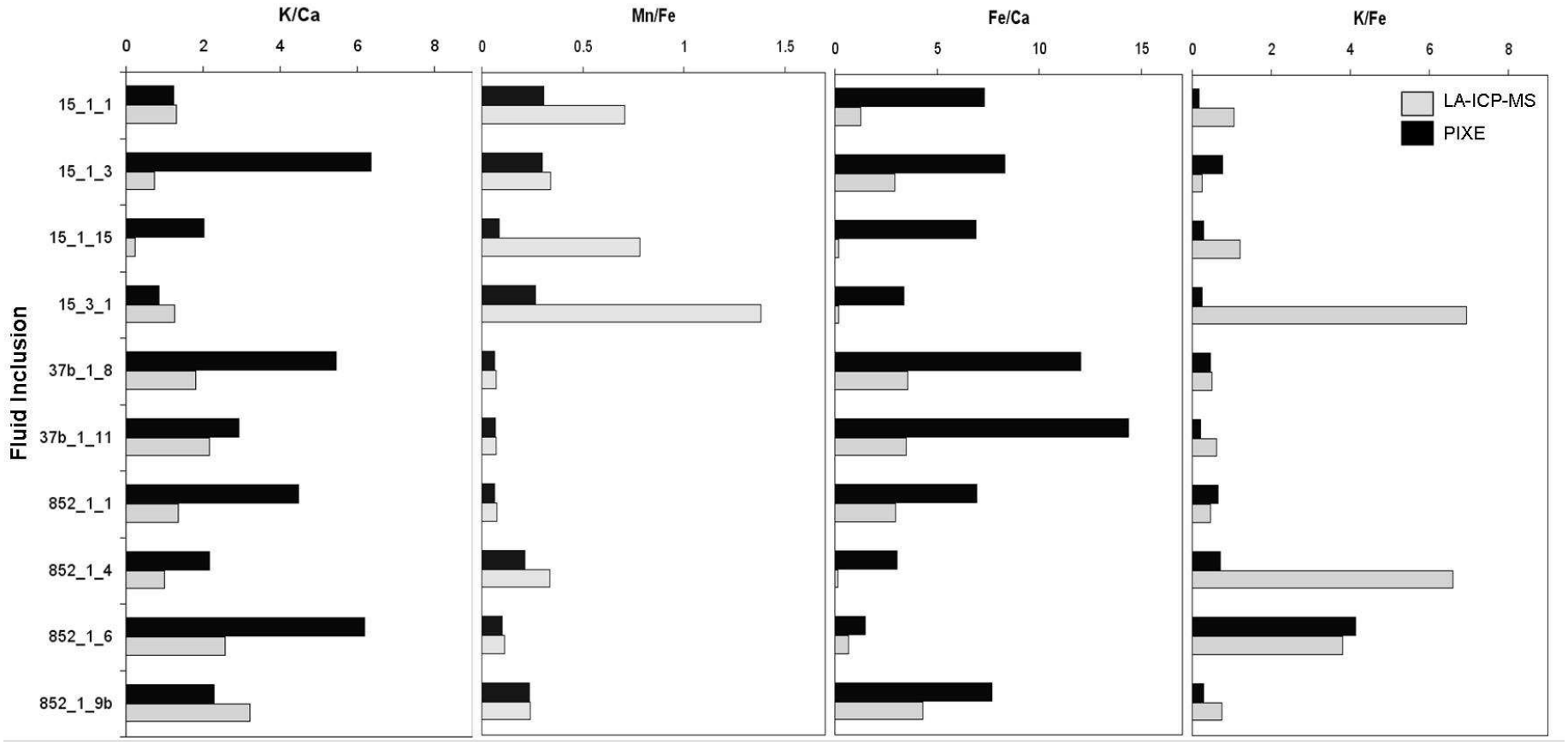

Figure 4.4 Comparison of selected element ratios in fluid inclusions measured by both PIXE and LA-ICP-MS.
Fe/Mn show strong similarity in values except for inclusions from sample Osb15 where there are low Fe concentrations suggesting LA-ICP-MS ablation of Fe-bearing solids may have been incomplete in these inclusions. While Fe/Mn and, to a lesser extent, K/Fe ratios show consistency between the two methods (with some exceptions, possibly the result of inefficient ablation of Fe-bearing solids by LA-ICP-MS, or addition to the Fe signal by ablation of small sulphide inclusions in quartz overlying the inclusion), K/Ca and Fe/Ca values suggest that Ca is disproportionately estimated by one of the methods.

Inclusion	Method	Concentration (ppm)											
		Cl	Na	K	Ca	Mn	Fe	Zn	As	Rb	Sr	Ba	Pb
15_1_1	PIXE	27762		4083	3281	7407	24012	468	1485	141	<120.	913	374
	LA-ICP-MS		*112137*	*36222*	*27628*	*24370*	*34487*	*3300*	*198*	*198*	*140*	*870*	*84*
15_1_3	PIXE	111334		28392	4469	11129	37100	2254	3482	<442.	413	2568	1565
	LA-ICP-MS		*138808*	*13307*	*17955*	*17885*	*52430*	*900*	*1074*	*161*	*160*	*2287*	*665*
15_1_15	PIXE	141565		23148	11399	6708	78566	945	1275	415	417	7676	436
	LA-ICP-MS		*126146*	*33634*	*139246*	*21845*	*27861*	*9750*	*1272*	*731*	*1963*	*1053*	
15_3_1	PIXE	442812		25198	29162	26270	98218	1902	<53.	913	1008	4405	1318
	LA-ICP-MS		*92217*	*129148*	*101597*	*25701*	*18593*	*11400*	*<247*	*1157*	*2915*	*14625*	*1873*
37b_1_8	PIXE	279500		49925	9171	7011	110232	1013	1009	478	921	1096	<428.
	LA-ICP-MS		*109694*	*42976*	*23792*	*6174*	*84803*	*1170*	*146*	*352*	*362*	*2122*	*190*
37b_1_11	PIXE	13485		9009	3088	3064	44381	390	167	255	221	667	167
	LA-ICP-MS		*104203*	*54090*	*24891*	*6310*	*87227*	*760*	*144*	*334*	*333*	*1769*	*149*
852_1_1	PIXE	175556		41638	9301	4000	64549	623	404	582	504	1564	596
	LA-ICP-MS		*107064*	*28388*	*20979*	*4593*	*62593*	*1160*	*124*	*332*	*349*	*2014*	*141*
852_1_4	PIXE	361031		54606	25295	16395	76638	2492	1334	546	200	<498.	1625
	LA-ICP-MS		*72981*	*25321*	*25532*	*1298*	*3835*	*8500*	*122*	*164*	*154*	*1750*	*1240*
852_1_6	PIXE	489061		88896	14366	2210	21507	396	654	423	374	1492	679
	LA-ICP-MS		*99861*	*108351*	*42109*	*3191*	*28442*	*9800*	*224*	*385*	*2060*	*4961*	
852_1_9b	PIXE	26118		3778	1648	2992	12675	377	675	117	<86.	<280.	233
	LA-ICP-MS		*130378*	*40316*	*12549*	*13029*	*54218*	*8000*	*638*	*429*	*150*	*509*	*2388*

Table 4.6: Inclusions analysed by both PIXE and LA-ICP-MS.
Inclusions 15_1_1, 37B_1_11 and 852_1_9b are CB inclusions with a significant CO_2 component. The low concentrations measured in these may indicate that estimates of fluid density are inaccurate or that the inclusion size and/or depth has been incorrectly measured, resulting in underestimation of concentrations. Element ratios are similar to those measured by LA-ICP-MS (Fig. 4.4). It has been noted that PIXE may overestimate As concentrations (section 4.2.1). The data is included here for comparison with LA-ICP-MS data. Comparisons suggest that the degree of overestimation is not systematic.

within 10% error of each other. Fe/Ca data for each inclusion show apparently systematic differences between values obtained by each method which suggest that PIXE analysis consistently underestimates Ca or overestimates Fe (or that LA-ICP-MS overestimates Ca and underestimates Fe).

The similarity in Mn/Fe values measured by both methods requires that if it is Fe that causes the variation, then Mn must be subject to the same problems, suggesting this discrepancy is due to errors in Ca analysis. The greatest disparity between measured ratios is observed in K/Ca values, suggesting that it is analyses of Ca concentration that show greatest variation between the two methods, although there is likely to be considerable noise in K data from PIXE analyses caused by the high sensitivity of the element to errors in depth estimates and by varying concentrations of K in the quartz host mineral (see Chapter 3, Table 3.5); PIXE element maps show high background K in some samples (Osb15; Fig. 4.1) and much lower K in other samples (Osb36; Fig. 4.1). PIXE analyses of Ca will also show high sensitivity to errors in depth estimates, due to greater attenuation effects on Ca X-rays with increased depth, and due to mass interferences with the argon carrier gas in LA-ICP-MS a low abundance isotope is analysed which may also lead to errors in calculated concentrations. However, as Fe/Ca ratios show a more consistent discrepancy, measurement of K can be considered to show greatest inconsistency between the methods. When PIXE and LA-ICP-MS data sets are compared for K/Ca values the PIXE values are generally higher than those from LA-ICP-MS (Fig. 4.4).

In the PIXE data set, inclusions from some samples show positive correlations between the concentrations of metals and Cl that will be partly due to systematic errors which

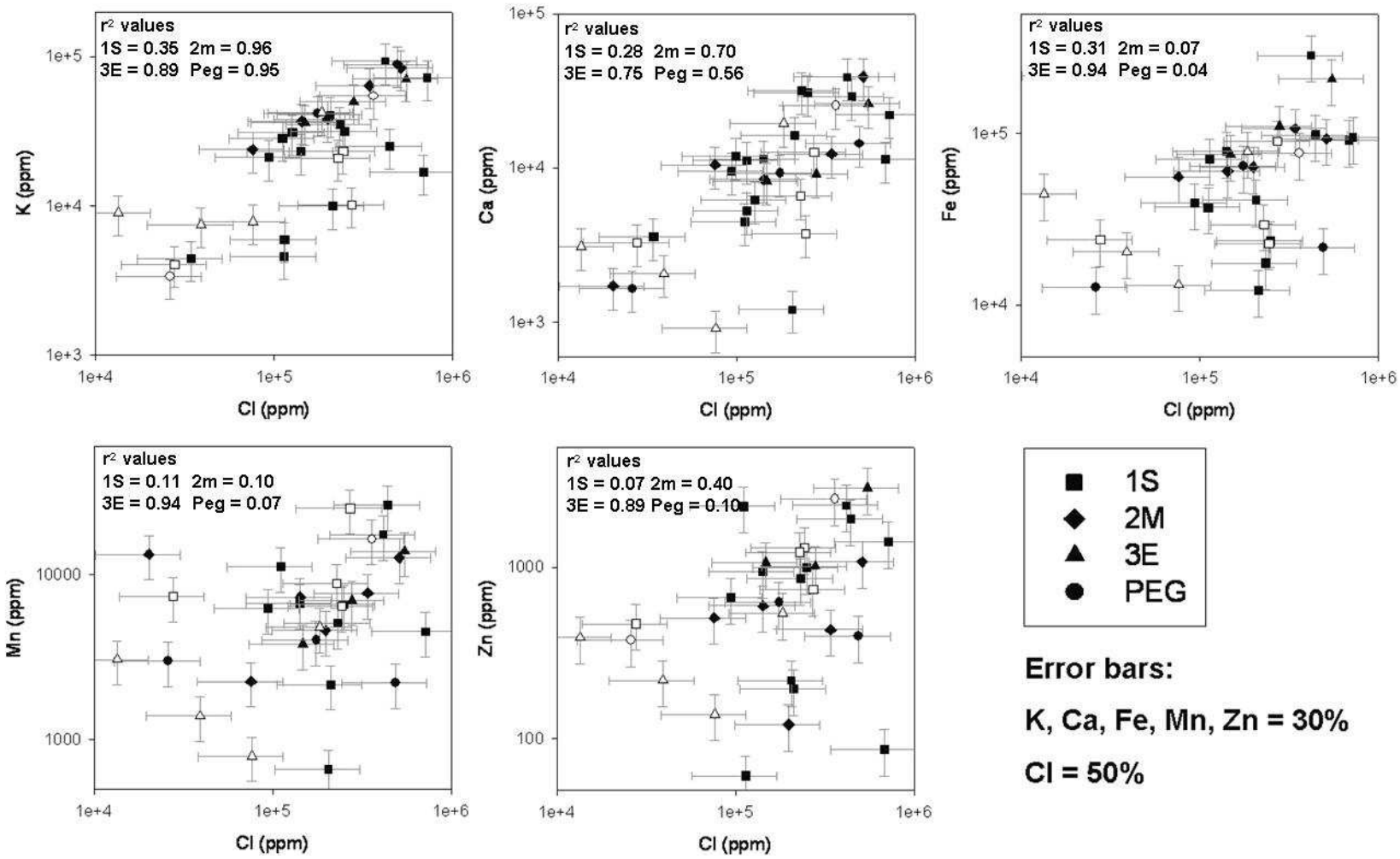

Figure 4.5: Cl vs metal concentrations in CB (open symbols) and MS inclusions (solid symbols).
For inclusions from 3E samples, all metals show a positive correlation with Cl (r^2 0.75 – 0.94). Inclusions in 2M samples also show positive correlations between Cl and K and Cl and Ca. Inclusions in other samples show weak or no correlation. Scatter around lower Cl concentrations may indicate attenuation of X-rays from lighter elements in deeper inclusions.

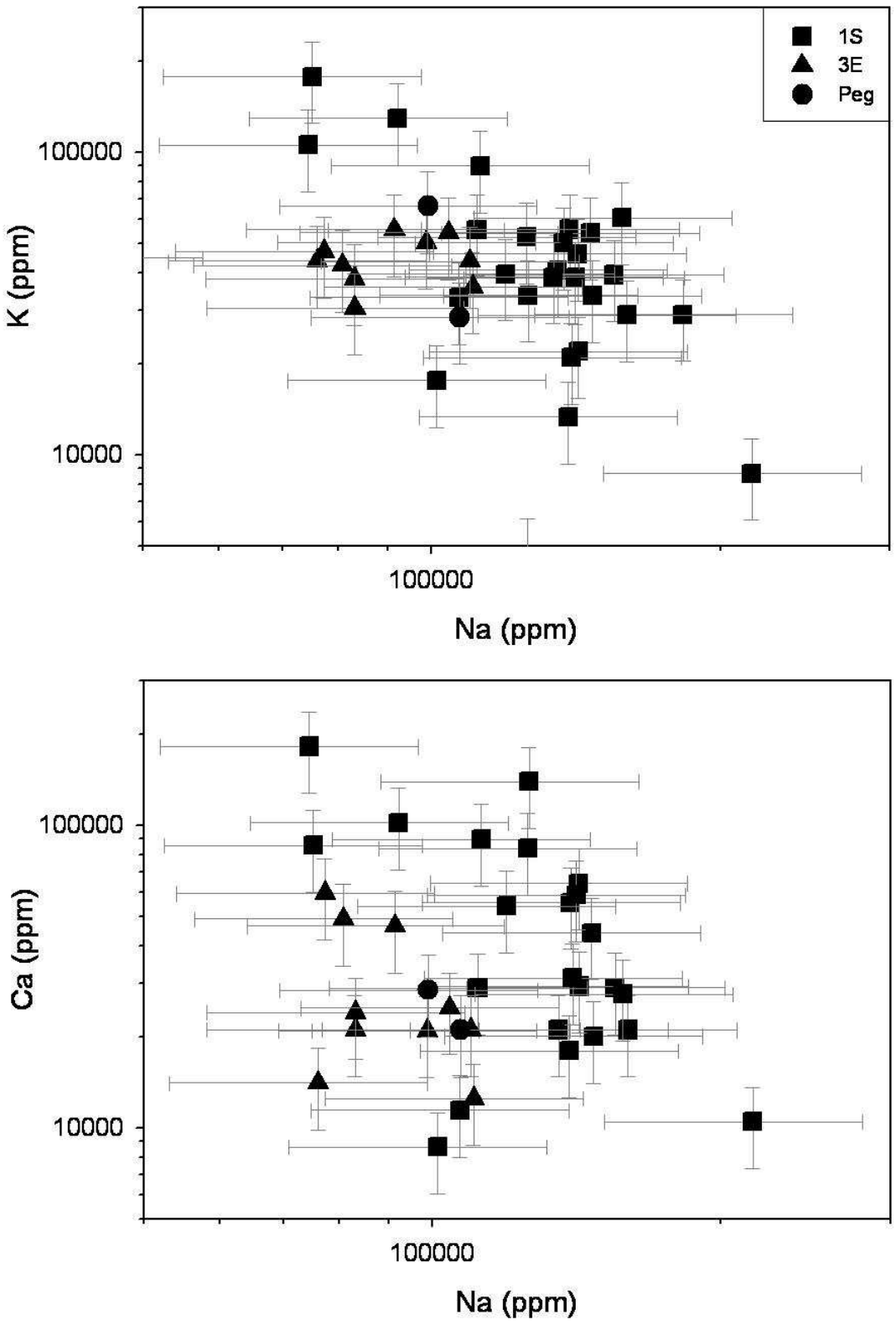

Figure 4.6: Correlations between major cation concentrations in inclusions analysed by LA-ICP-MS A weak negative correlation is observed between K and Na, with no correlation observed between Ca and Na. Over an order of magnitude variation in concentrations are observed for all three elements (although, allowing for errors, the variation may be less)

affect all elements similarly (Fig 4.5). However there are differences in cation proportions within the inclusions (Table 4.2; 4.4). In the LA-ICP-MS data the cations show considerable variation with a strong negative correlation between K and Na and a weaker negative correlation between Ca and Na (strongest in 1S samples, less obvious in 3E and Pegmatite samples; Fig. 4.6). PIXE element mapping shows there is considerable variation in element phase association; most notably with Ca, Ba and Zn which are observed bound in solid phases in some inclusions and are dissolved in the liquid phase in others (Fig. 4.1). Ca and Ba (where present) appear to be bound in a solid phase within the CO_2-bearing CB inclusions and dissolved in the liquid phase within MS inclusions. A Ca-bearing solid (presumed, based on laser Raman analyses to be calcite – see section 2.3.2) is observed in all but one of the 12 CB inclusions analysed by PIXE (see Appendix E; H). A clear Ba signal is only identified in four of the CB inclusions, in three cases associated with the calcite. In most inclusions Ba/Ca ratios are less than 0.3. The much higher concentrations of Ca than Ba (in many inclusions over an order of magnitude) suggest that the Ba substitutes into calcite at low levels. However, given that calcite and witherite are not isomorphous, at higher concentrations of Ba it is probable that $BaCO_3$ will exceed its solubility in calcite and that the solid is either an amalgam of the two salts. In sample 15_1_1 (a CB-type inclusion) a Ba-bearing solid, distinct from the calcite solid, is assumed to be a barium carbonate.

Both PIXE and LA-ICP-MS show that the inclusions contain very high Fe concentrations (up to 17 wt %). Many of the inclusions also have high concentrations of Mn (up to 4 wt %) and Mn/Fe is variable, from 0.04 to >0.32, with the variation having a relationship to sample location (Fig. 4.7). Within the LA-ICP-MS data set, the

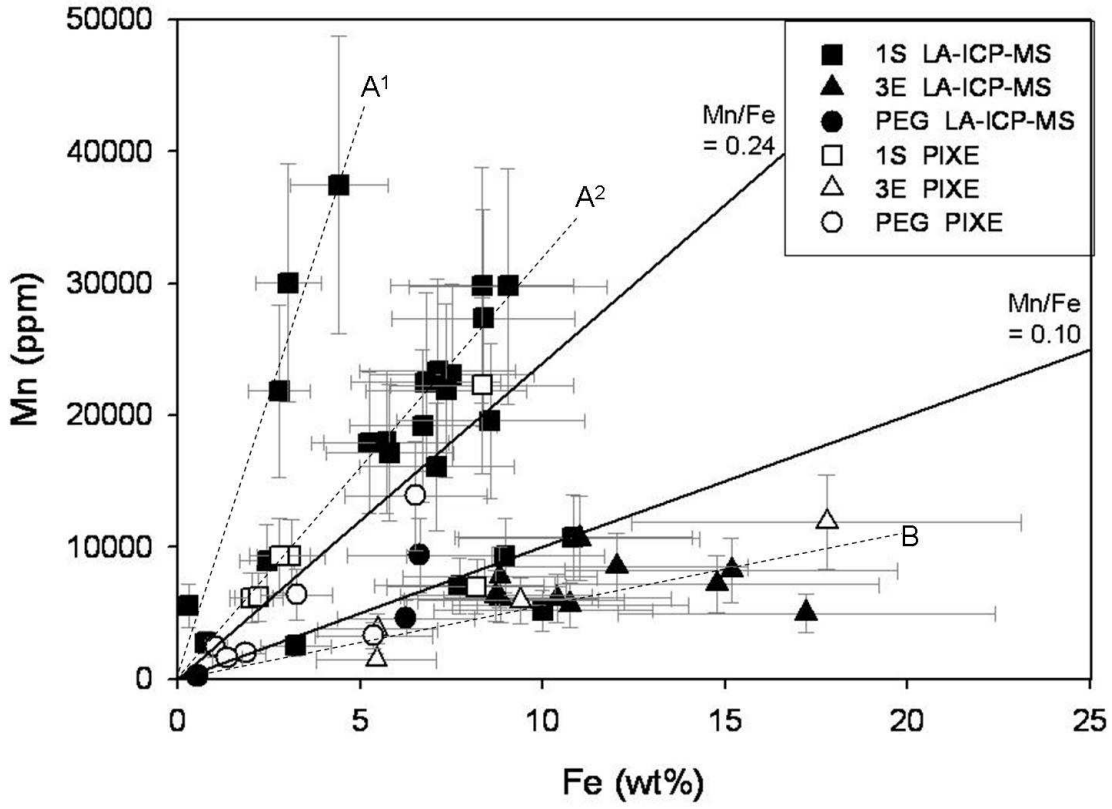

Figure 4.7: Mn/Fe values in CB and MS fluid inclusions. Values show an association with the redox state of the host mineral assemblage. Bottrell and Yardley, (1991) suggested reduced (pyrrhotite-associated) fluids have Mn/Fe values of less than 0.24. Within the Osborne samples 3 different populations of Mn/Fe values can be distinguished. The majority of the fluids sampled in the chalcopyrite-pyrite ore zone have Mn/Fe values above 0.24 with group A^1 having Mn/Fe values of 0.86 and group A^2 having Mn/Fe values of 0.32. Fluids in the reduced pyrrhotite-rich ore zone have Mn/Fe values below 0.1, with group B having Mn/Fe values of 0.06. This association implies that the high salinity MS and CB brines are primary ore fluids.

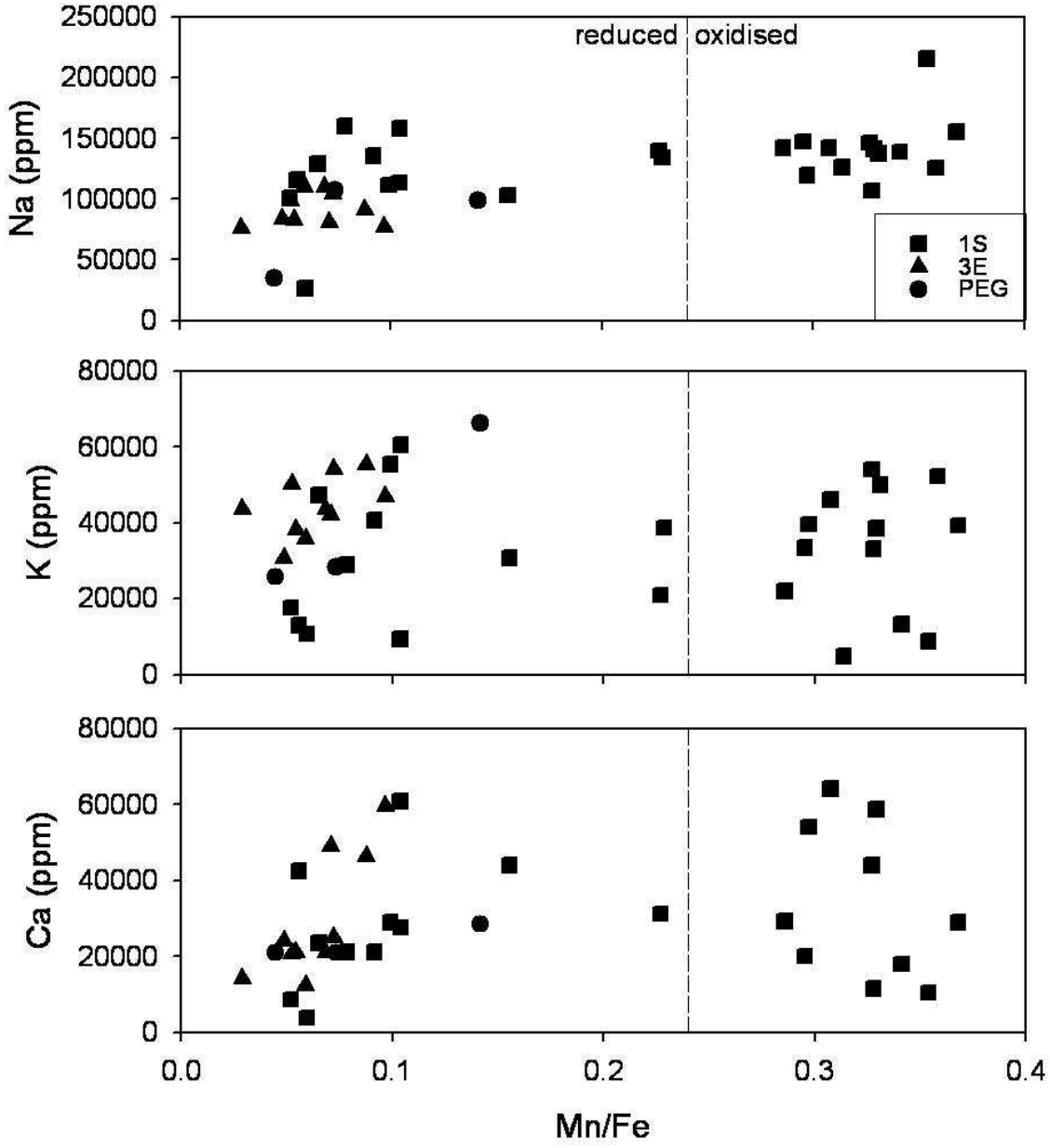

Figure 4.8: Mn/Fe values vs major cation concentrations. LA-ICP-MS data shows fluids from the 3E ore lens with low Mn/Fe (<0.24, inferred to be reduced fluids; Bottrell and Yardley, 1991) have a weak to moderate positive correlation (r^2 0.32 – 0.62) between Mn/Fe values and Na, K and Ca concentrations with no correlation observed for 1S and Pegmatite samples. Fluids with Mn/Fe greater than 0.24 (suggested to be oxidised fluids; Bottrell and Yardley, 1991) do not show the same trend. Data for other elements present at lower concentrations including Cu, Zn, Pb have too much scatter for similar trends to be identified.

Mn/Fe ratios define two groups of inclusions; one with Mn/Fe below 0.1 and the second with Mn/Fe above 0.24. In the former group, weak positive correlations between Mn/Fe and Na, K and Ca are observed for samples from the pyrrhotite bearing 3E lens (Fig 4.8) whereas in the latter group and 1S and Pegmatite samples such a correlation is not obvious.

The Cu-signal in many inclusions is exaggerated by a Fe-Si X-ray pulse pile-up which artificially contributes to the measured Cu concentrations (see section 4.2.1). Once this effect is removed, in almost all cases the measured Cu is below the detection limit for the method (typically <100ppm). The low Cu content of the ore fluids is confirmed by LA-ICP-MS studies with the majority of analyses measuring Cu concentrations below 100ppm. One sample gives an outlier value of 925ppm (Appendix F), but this could be attributed to the contribution of a Fe-Cu-sulphide grain within the matrix, accidentally sampled during ablation, with a very high Fe concentration also measured. Although the PIXE element maps of MS fluid inclusions suggest Cu is associated with Fe-bearing minerals, where Cu is actually detected it appears to be mainly dissolved in the brine phase (Fig 4.1; Appendix H).

In element X-ray maps Zn is associated with the Fe- and Mn-bearing solid or solids (Fig. 4.1). Pb and Rb also show an association with Fe-bearing minerals but as these elements would not be expected to substitute into Fe-silicates, this is identified as an artificial signal caused by high Fe-concentrations raising background levels across the spectrum. While the effects of this iron noise are observed in the element maps the GeoPIXE program removes the predicted noise from the final data sets. In most inclusions the Fe-bearing solid is ferropyrosmalite ($(Fe,Mn)_8Si_6O_{15}(OH,Cl)_{10}$), although

a limited number of inclusions contain an opaque solid believed to be magnetite. The presence of ferropyrosmalite indicates the presence of reduced Fe^{2+} (ferrous) iron, which is much more soluble than Fe^{3+} (ferric) iron (Bottrell and Yardley, 1991), and, thus, correlates with the low Mn/Fe measured for inclusions with highest iron concentrations.

Nearly two orders of magnitude variation in Br/Cl values were measured with values between 0.14×10^{-3} and 18×10^{-3} (Fig. 4.9). Samples from the 1S ore zone have the highest values while maximum values measured in the pegmatites, 2M and 3E zones are $<2 \times 10^{-3}$. Anomalously high Br concentrations are measured in CB (and one MS) inclusions from sample Osb15 which is from the deep part of the 1SS ore zone. The Br is not associated with any solid phase. In general, the fluid inclusions from sample Osb15 have compositions that are distinct from the majority of other inclusions analysed, and have low K, and high Zn (Table 4.2). Br/Cl values measured in both CB and MS inclusions have a similar range of variation, and although CB inclusions from the 1S lens plot in a distinct cluster, their values are within the range measured in MS inclusions from the same samples.

K/Ca values span a broad range of over an order of magnitude in all ore zones, from 0.2 to 8 (Fig. 4.10). Highest values are measured in PIXE samples and the majority of PIXE analyses plot above LA-ICP-MS analyses. The variation between PIXE and LA-ICP-MS K/Ca values can not be attributed to errors in estimating inclusion depth for PIXE analyses. Modelled effects of wrongly estimated depths using GeoPIXE software suggests that errors in fluid inclusion depth estimates of 1μm will typically result in less

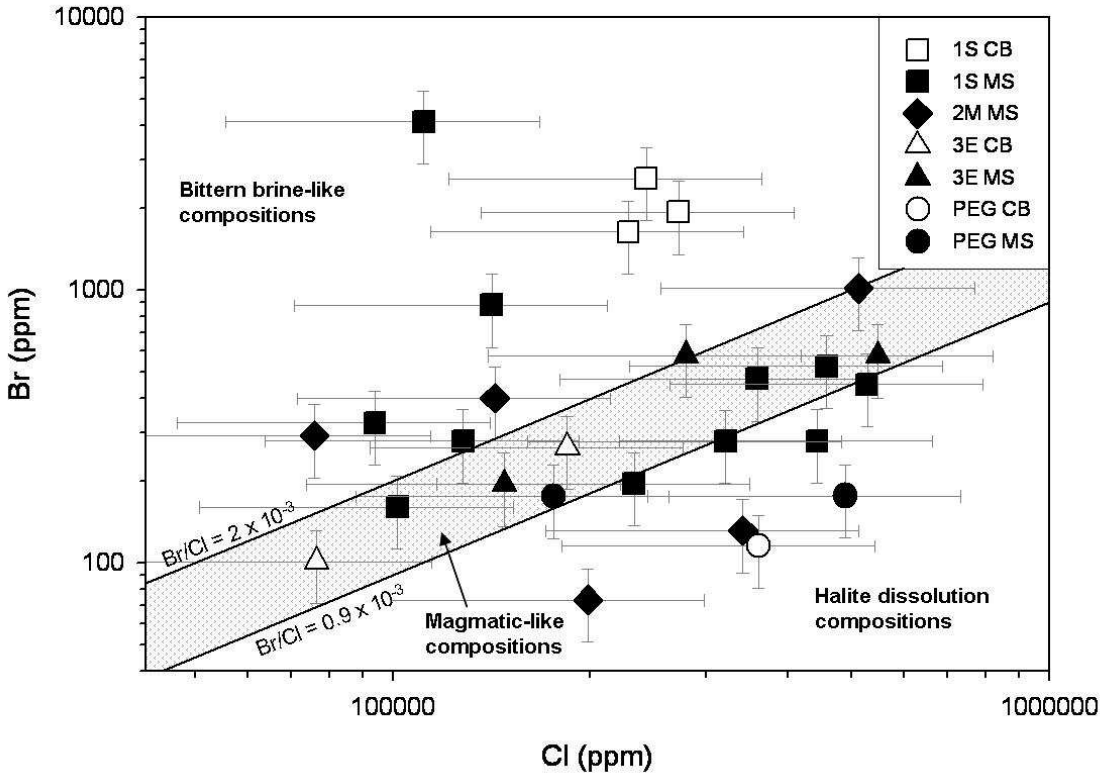

Figure 4.9: Br vs. Cl measured by PIXE. Br/Cl values have more than two orders of magnitude variation, with some fluids having a composition consistent with evaporite dissolution while other fluids have values that plot in the bittern brine field or higher, suggesting metamorphic processes may have influenced the halogen chemistry through uptake or release of Cl during metamorphic reactions. Only a few values plot in the field of magmatic-like compositions and these values can be accounted for by mixing between the two end-member compositions, suggesting a magmatic fluid component is absent or limited. CB and MS inclusions have similar ranges of Br/Cl values. Error bars = 30% for Br, 50% for Cl.

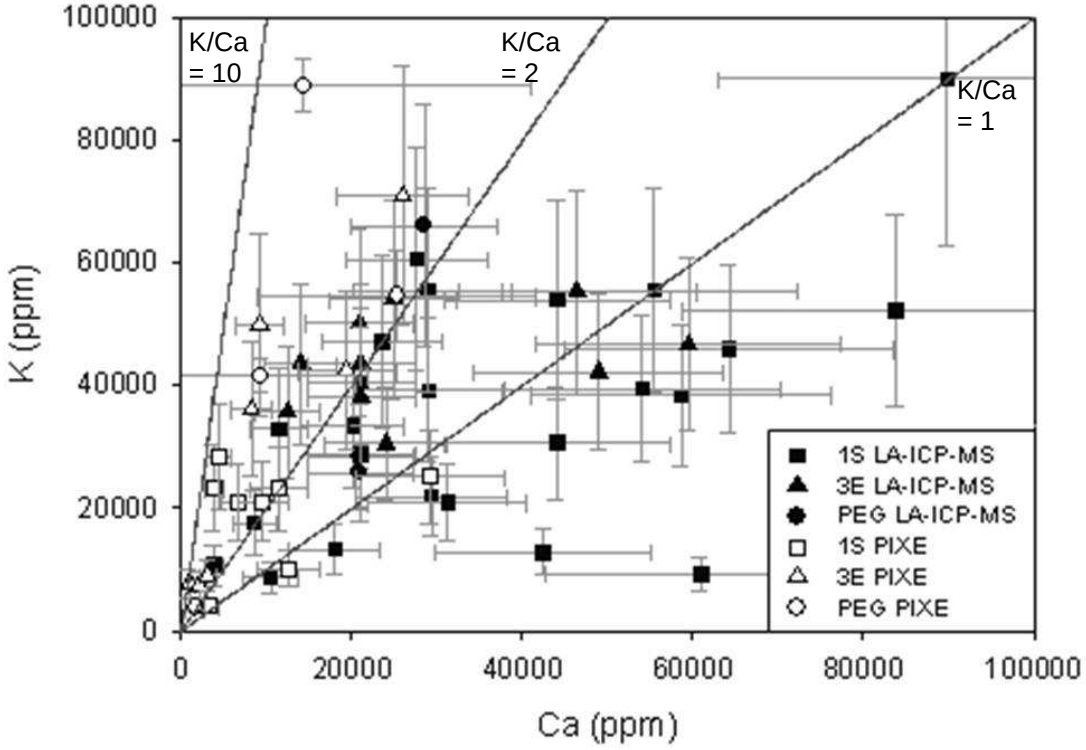

Figure 4.10: K vs Ca measured by PIXE and LA-ICP-MS.
K/Ca values show more than 2 orders of magnitude variation with values measured by PIXE mostly higher than those measured by LA-ICP-MS. Errors bars = 30%.

than 5% change to the K/Ca value, for both deep and shallow inclusions in the Osborne samples. However, deeper inclusions will be more susceptible to errors caused by K in the quartz host as the magnitude of this signal relative to the K signal of the inclusion increases.

4.3.1 Comparison of micro-analytical methods

Two micro-analytical techniques, PIXE and LA-ICP-MS have been used to study the same set of samples from the Osborne mine. The data from each type of analysis shows similar elemental ratios. However, each method has advantages and the use of the two together permits greater resolution of the fluid chemistry. In particular the identification of element and phase associations is an advantage of using PIXE while the lower detection limits of the LA-ICP-MS method provided information on low Cu concentrations which are below the PIXE detection limits.

Both techniques were used to study MS inclusions, and for almost all samples, higher concentrations were measured by LA-ICP-MS for most major fluid components. Measured PIXE concentrations of cations including Ca, Ba, Mn, Pb and Zn are significantly lower than in LA-ICP-MS analyses of similar inclusions (Table 4.6). A lesser disparity between methods is observed in measurements of trace elements such as Rb and Sr. This could suggest that PIXE, as applied here, variably underestimates concentration, and thus a correction is required to calculations using X-ray attenuation or to the fluid inclusion geometry model used to model concentrations. Or it may imply that microthermometric estimates of salinity (in NaCl wt % equiv.) used to reduce the LA-ICP-MS data were too high and did not take account of the complex salt system.

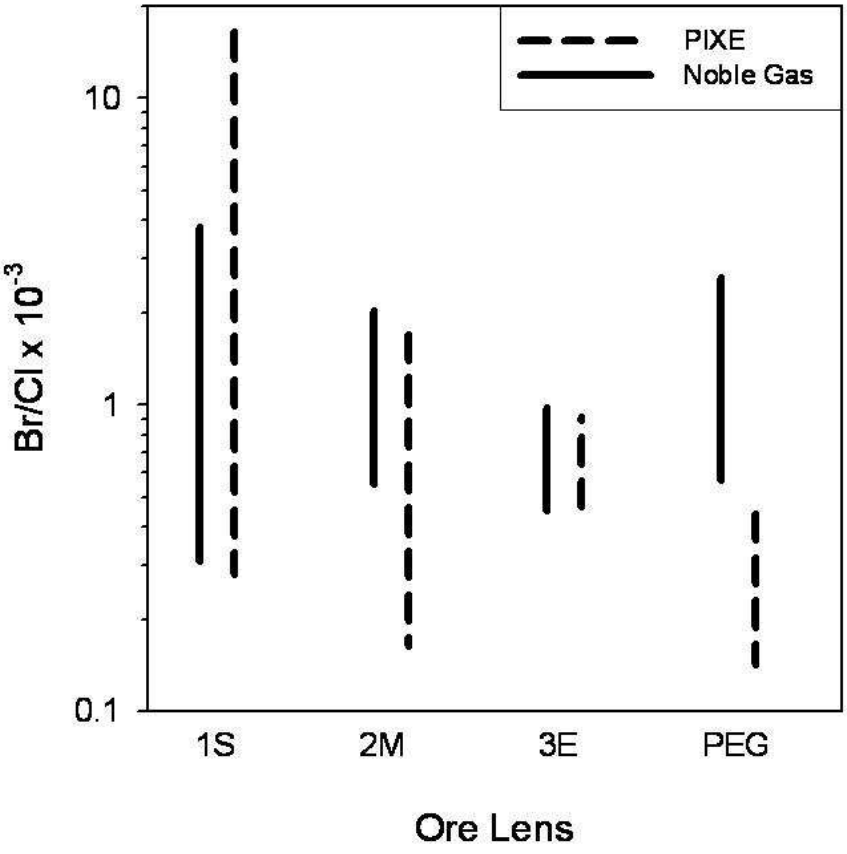

Figure 4.11: Comparison of range of Br/Cl values obtained by PIXE and combined noble gas and halogen analysis.
Values measured in samples from the three ore zones show overlapping ranges with values measured by PIXE having more outlying values. The range of values measured in pegmatite samples by each method do not overlap. This is probably a function of the proportion of each fluid inclusion population present within the sample; while measurements from PIXE are taken from individual MS and CB inclusions the noble gas and halogen analysis is semi-selective technique and thus the data represents the mixed contents of MS, CB and LVD inclusions.

Once the element ratios are calculated the PIXE and LA-ICP-MS data are mainly compatible (Fig. 4.4). Where fluid inclusions were analysed by both methods the greatest discrepancy was in the measurement of Ca. If the PIXE analyses are normalised to K measured by LA-ICP-MS similar element concentrations are identified. The consistently lower values measured for all elements by PIXE suggest that fluid inclusion depths may have been underestimated while fluid salinities were overestimated for LA-ICP-MS.

Both PIXE and LA-ICP-MS have problems associated with Ca analysis. Due to mass interferences associated with the argon carrier gas in LA-ICP-MS Ca is analysed by measuring ^{43}Ca, a minor isotope, and the overall Ca extrapolated from natural isotope ratios. Due to the low concentrations of ^{43}Ca this introduces errors into the analysis. PIXE analyses can also incur errors associated with errors in depth calculations and attenuation of signals in inclusions at depths greater than 15μm. This particularly impacts on the measurement of lighter element such as Cl, K and Ca. When concentrations of K and Ca are plotted against inclusion depth, only low concentrations are measured in inclusions at depths greater than 6μm (Fig 4.12). Low concentrations are measured for some shallow inclusions, however the majority of these are CB-type inclusions, which suggests that high volumes (>15 % by volume) of high density CO_2 may dilute the measured concentrations. When elements, such as Ca and K, that show X-ray attenuation with depth, are ratioed against an element, in this case Zn, that does not have attenuation with depth a negative correlation is observed for Zn/Ca and Zn/K plotted against increasing depth, particularly for MS inclusions (Fig. 4.13). As both elements are affected to a similar degree by the attenuation the K/Ca ratios can still be useful.

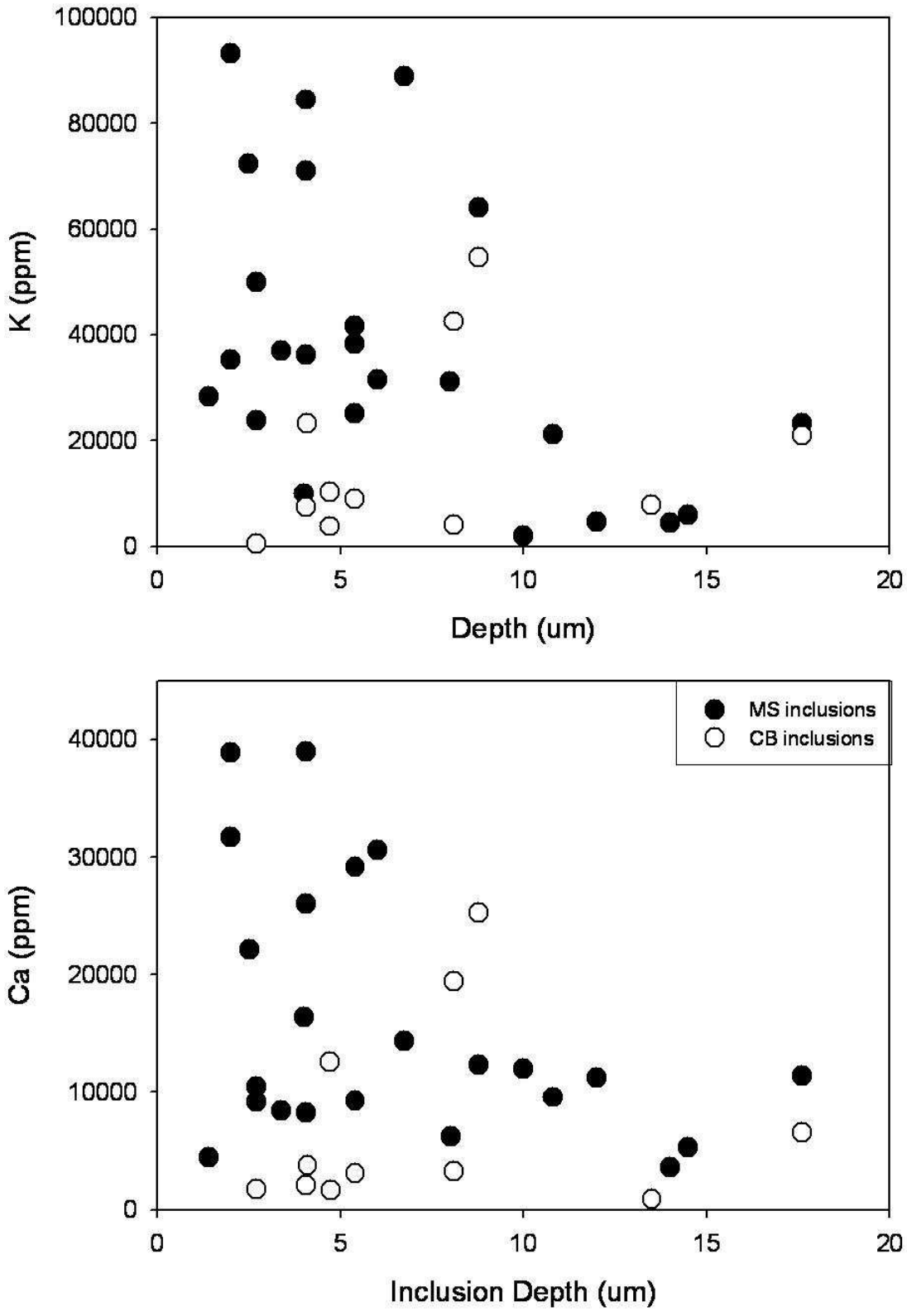

Figure 4.12: PIXE measured K and Ca concentrations vs. inclusion depth
A decrease in Ca and K is noticed with increased fluid inclusion depth, suggesting depths may have been underestimated.

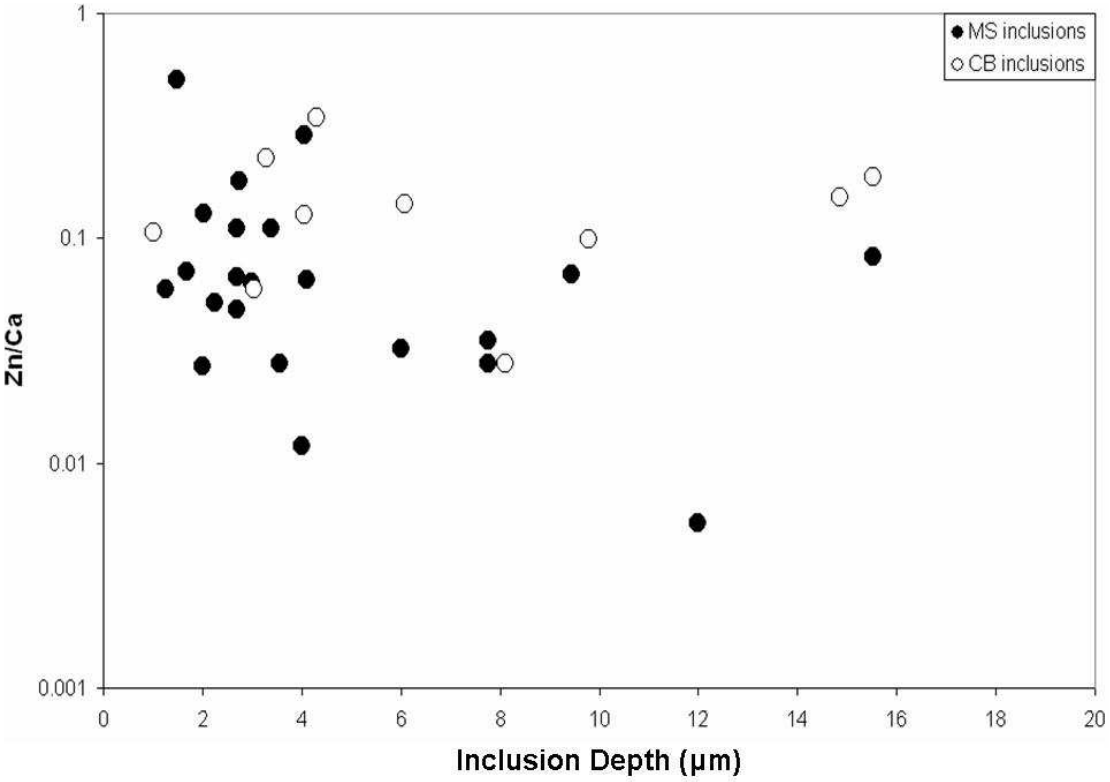

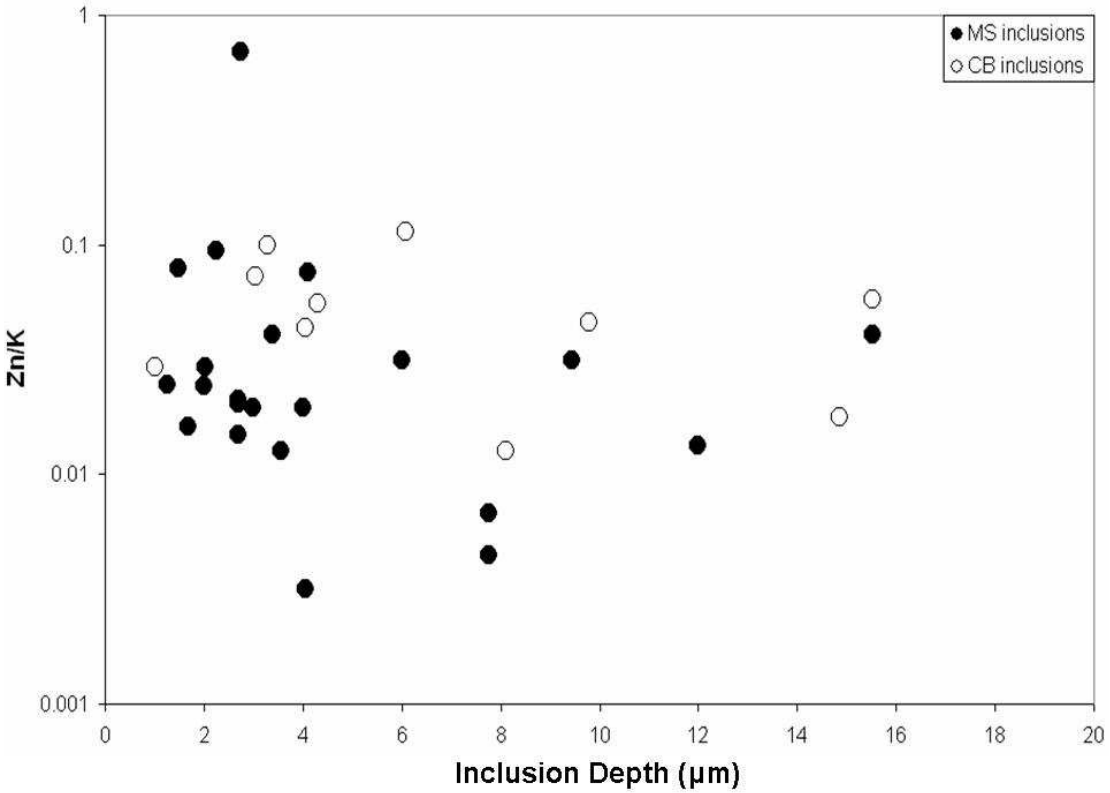

Figure 4.13: Zn/Ca and Zn/K vs. inclusion depth.
Element ratios show variation with increasing depth. While Ca and K X-rays attenuate with depth while Zn X-rays do not to anything like the same extent. The GeoPIXE software makes calculations for this effect, where fluid inclusion depth has been calculated correctly. So the negative correlation observed in this graphs, particularly for MS-type inclusions suggests, that for some inclusions the fluid inclusion depth may have been underestimated.

4.4 Discussion

4.4.1 Fluid Compositions

The primary Osborne ore fluids, preserved in MS inclusions, have salinities that are at the upper end of the range of hydrothermal brines documented in ore deposit studies (see Yardley et al., 2000; Yardley, 2005), similar to values measured in I-type magmatic fluids. The high salinities measured in many magmatic fluids are thought by many to reflect vapour loss from the fluids (Cline and Bodnar, 1994; Ulrich et al., 2001). However, the data from the conservative noble gas and halogen species do not support such an origin for the Osborne fluids (Chapter 3).

The ultra-high salinity fluids entrapped within MS inclusions are Fe- and Mn-rich with maximum Fe concentrations (of 17 wt% measured in MS inclusions from the 3E ore zone) similar to, and in some cases, exceeding by up to an order of magnitude Fe concentrations measured in high temperature magmatic fluids from other systems (Yardley et al., 2000; Ulrich et al., 2001; Rusk et al., 2004). These high concentrations are similar to those measured in other IOCG deposits in the region (Williams et al., 2001; Oliver et al., 2004) and can be considered the source of Fe in the sulphide ore minerals.

While the conservative elements such as Cl, Br and Ar can preserve information on fluid sources the concentrations of most other metals dissolved in a brine will be altered by fluid-rock reactions during transport. Fluid temperature is a strong control on these reactions with Na/K ratios typically having an inverse relationship with temperature. High temperature fluids of magmatic origin are often K-rich with low Na/K ratios, ranging between 0.5 and 7 with a mean of ~2.5 (Yardley et al., 2000; Rusk et al., 2004).

The Osborne ore fluids, however, are dominated by Na, with average Na/K values of 4 and maximum values of 25 (Table 4.5; Appendix F). This may be a function of temperature, with the Osborne fluids reaching maximum temperatures of 600-700^{o}C, while magmatic fluids may equilibrate at temperatures of 700-1000^{o}C.

As discussed in Chapter 3 the Br/Cl values of the fluids indicate that much of the Cl in the fluids was derived from the dissolution of evaporites (also see section 4.4.5). The composition of such fluids is typically dominated by NaCl (Kesler et al., 1995; Yardley et al., 2000) which may explain the low K/Na values. Alternately, Rubenach et al., (in press) have documented early (pre-1600Ma) albitisation of the host rock sequence at Osborne. If the host rocks were hotter than the fluids at the time of mineralisation then ore fluids would have interacted with the local wall-rocks which would have been Na-rich, possibly lowering K/Na ratios in the fluids.

K/Ca is variable in all ore zones, suggesting it is influenced by fluid rock reactions such as creation and destruction of muscovite and biotite, both of which form part of the gangue assemblage (see Table 1.2; Fig. 2.1). Selvages of biotite alteration are observed around the zones of silica flooding (Adshead, 1995). Formation of these would have removed both K and Fe from the fluid, potentially changing both K/Ca and Mn/Fe values. Potassic alteration of albitic pegmatites has been documented by Rubenach, (2005a), which would also impact on K/Ca ratios in the fluids.

Fe concentrations in fluids have also been shown to be temperature dependent with highest concentrations measured in high temperature magmatic brines (Yardley et al., 2000; Yardley, 2005). However this association can be considered to be a function of

temperature, rather than provenance. In a compilation of brine compositions, non-magmatic brines are only shown at temperatures <300^{o}C (Yardley et al., 2000). The noble gas and halogen data provide strong evidence for a non-magmatic origin for the ore fluids at Osborne (Chapter 3). Their moderate to high temperatures (documented by microthermometry; Chapter 2) are a result of the depths and pressures under which ore formed and thus their high salinities and high metal contents could be similar to those in fluids recognised as being of magmatic origin, due to similarities in physiochemical conditions.

4.4.2 Compositional similarities between brines in CB- and MS-type inclusions

No significant distinctions between cation concentrations and ratios in the brine phase of CB and MS inclusions are observed. Some variation is observed in the associations of Ba and Ca. The two elements have been observed to be bound in solid phases at room temperatures within CB inclusions (Fig 4.1; Appendix H). Laser Raman studies of CB inclusions have also identified calcite as a daughter mineral suggesting that Ca and Ba are bound in a carbonate phase where the fluid inclusion is CO_2-bearing. The much higher concentrations of Ca (>5-10 times greater) than Ba indicate this daughter mineral is not a specific Ba-Ca-carbonate such as barytocalcite but rather suggest Ba may be a minor component substituting for Ca in the calcite structure. $BaCO_3$ generally forms in the aragonite structure but laser Raman spectroscopy which is effective at distinguishing between calcite and aragonite (Behens et al., 1995; Anderson, 1996) confirm that the carbonate mineral is calcite (Chapter 2). Barium can be incorporated into calcite in defect sites or directly substituting for Ca (Pingitore, 1986; Reeder et al., 1999), but at higher concentrations of Ba the coprecipitation of witherite and calcite is

more probable. In the absence of CO_2 the two elements remain in the liquid phase at room temperature (e.g. in MS inclusions).

There is compositional variation between the brines trapped in both CB and MS inclusions but there are no systematic differences between the two inclusion types, with the same ranges of element ratios observed in both populations. It has been suggested that a homogenous CO_2-bearing brine (the fluid entrapped within CB inclusions) unmixed, creating a high salinity brine, as observed in MS inclusions, and a separate CO_2 fluid (Mustard et al., 2004; Chapter 2). The similarities between the brine phases entrapped in each inclusion type support unmixing with the fluid in MS inclusions derived from that in CB inclusions and no significant fractionation of any measured element by the separating carbonic phase.

4.4.3 Copper concentrations and solubility in the ore fluids

The MS and CB fluid inclusions are primary inclusions in the main phase of silica flooding, which cathodoluminscence has shown predates the majority of sulphide deposition. Thus, the MS and CB inclusions can be considered to contain the pre-deposition primary ore fluids which became saturated with respect to chalcopyrite at low Cu concentrations. Low Cu concentrations in MS inclusions could be interpreted as evidence the fluid had precipitated chalcopyrite before entrapment, however, petrographic studies of the fluid inclusion assemblage (Chapter 2) have shown that the lower salinity LVD inclusions lie on trails that radiate from chalcopyrite grains, which suggests they represent the post-depositional ore fluids and the fluids trapped in MS inclusions can be considered pre-ore.

The high salinity and high temperature (~600^{o}C) Osborne ore fluids would have had the capacity to dissolve high concentrations of Cu, although Cu availability, sulphur content and oxygen fugacity will also limit copper solubility. Therefore, the low concentrations measured in pre-ore fluids at Osborne indicate the fluids may have been undersaturated with respect to Cu. However, the concentrations in the pre-ore fluids are above minimum values of ~10 ppm estimated to be required to form base metal deposits (Seward and Barnes, 1997).

The low Cu concentrations in the Osborne fluids raise questions as to how these fluids reached saturation with respect to Cu, triggering chalcopyrite deposition. Studies of copper complexing in hydrothermal fluids (Seyfried and Ding, 1993; Hezarkhani et al., 1999; Ulrich et al., 2001; Liu and McPhail, 2005) have demonstrated temperature is a major factor controlling chalcopyrite solubility and deposition. At 1kbar, a decrease in temperature from 500 to 300^{o}C in a 10 molal chloride solution (9:1 NaCl : KCl, corresponding to 37 wt% NaCl) results in a large decrease in chalcopyrite solubility, from 273ppm to 1ppm in solutions buffered by a hematite-magnetite-pyrite assemblage and from 128ppm to 0.5ppm in magnetite-pyrite-pyrrhotite buffered solutions (Liu and McPhail, 2005).

Cooling of Cu-bearing fluids to below 400 ^{o}C has been suggested to be the cause of chalcopyrite precipitation at the Starra IOCG deposit and Bajo de la Almubrera porphyry deposit (Ulrich et al., 2001; Williams et al., 2001; Liu and McPhail, 2005). A similar cooling of fluids is documented at Osborne with the primary fluids in MS inclusions trapped at temperatures between 300 and 600 ^{o}C, while the secondary LVD inclusions, containing post-deposition fluids, were entrapped at temperatures between

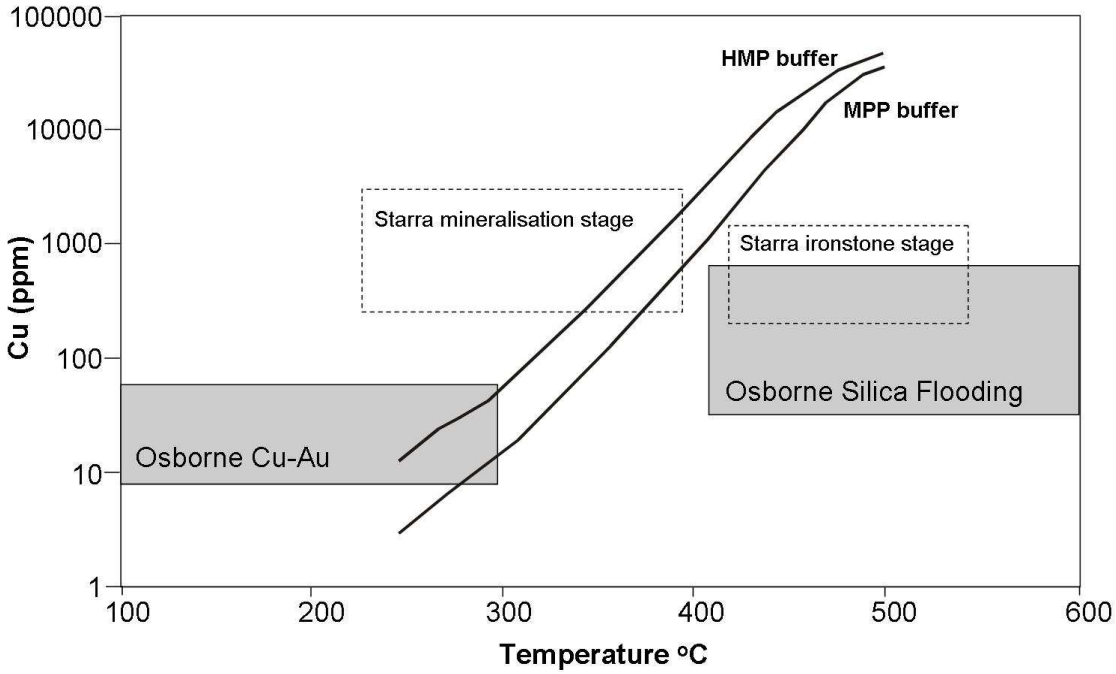

Figure 4.14. Comparison between calculated chalcopyrite solubility and Cu concentrations measured by PIXE and LA-ICP-MS at the Osborne deposit (modified after Liu and McPhail, 2005). The solid lines denote calculated chalcopyrite solubility in 10 molal chloride solutions (equivalent to 37 wt% NaCl – similar to highest values measured in post deposition LVD inclusions at Osborne) at 1 kbar in equilibrium with hematite-magnetite-pyrite (HMP) and magnetite-pyrite-pyrrhotite (MPP). The grey shaded boxes represent the measured ranges of homogenization temperatures and Cu concentrations measured in pre- and post-ore deposition fluids at the Osborne deposit. Data from the Starra deposit are given for comparison (Williams et al., 2001).

98 and 292 ^{o}C (Section 2.4.3). A comparison of the Starra data with that from Osborne shows that cooling of the Osborne ore fluids could have caused chalcopyrite saturation and deposition (Fig 4.14). The effects of pressure on Cu solubility are less clear. Studies report higher predicted chalcopyrite solubility with decreased pressure (Hemley et al., 1992; Liu and McPhail, 2005), however, this effect is neglible compared with temperature effects. The extensive silica-flooding observed at Osborne may be the result of rapid decompression associated with fracturing (see Chapter 2), and the unmixing of the early mixed brine-carbon dioxide fluid entrapped within CB inclusions to form separate brine and carbonic phases is postulated to be the consequence of a decrease in pressure (Chapter 2.5.3). However increased solubility as a result of these processes would be counteracted by the cooling recorded in the fluid inclusion assemblage at Osborne. Other factors such as changes in redox conditions, chlorine concentrations and pH are also controls on Cu solubility. Decreases in f_{O_2} and Cl^- concentrations will lead to decreases in Cu concentrations while decreased pH increases Cu concentrations. The loss of CO_2 during phase separation of the CB fluid would increase the pH of the residual brine, reducing Cu solubility.

Processes such as fluid mixing and fluid-rock reactions may also result in changes to the physiochemical conditions of the fluids, causing chalcopyrite deposition (Woitsekhowskaya and Hemley, 1995; Liu and McPhail, 2005). Microthermometric studies of Osborne document a decrease in fluid temperature and salinity over the evolution of the deposit which has been attributed to fluid mixing (Adshead, 1995; Section 2.5.3) which could have resulted in changes to Cl^- concentrations and pH. Experimental data from synthetic fluid inclusions suggest that mixing processes are not

significant above 500 ^{o}C where high temperatures control Cu solubility but may be important at lower temperatures (Hack and Mavrogenes, 2006).

While low Cu concentrations (<200ppm) are measured in both pre- and post-depositional fluids, other base metal concentrations, particularly Zn and Pb are higher despite these elements not being represented in the ore mineral assemblage. These elements become concentrated in the post-deposition ore fluids, relative to other elements, indicating that conditions were not suitable for their precipitation.

Experimental studies of the solubility of Fe-Cu-Zn-Pb sulphides in ore-forming systems show that all the solubilities increase with increasing temperature and chloride concentrations and decrease with increasing pressure (Hemley et al., 1992). Cu-Zn-Pb metal zoning is observed in porphyry copper deposits and other ore deposit types, a result of deposition on different saturation surfaces controlled by factors such as sulphur availability and metal concentrations (Hemley and Hunt, 1992). Experimental data also confirms that ZnS and PbS solubilities are higher than for Cu-sulphides, so that Pb and Zn will remain in solution when Cu precipitates. High Pb and Zn concentrations, exceeding that of Cu, are measured in ore fluids at Cu deposits, such as porphyry copper deposits (Ulrich et al., 2001; Rusk et al., 2004). The Zn/Pb values measured in the Osborne fluids are within the range that would be expected in brines equilibrated with rocks or magmas (Yardley, 2005).

Studies of fluids associated with Cu deposits, interpreted as having exsolved directly from magmas, have shown that high salinity fluids can transport high concentrations of Cu, with 1 to 2 wt% Cu measured in primitive magmatic fluids (Perring et al., 2000;

Ulrich et al., 2001). The Cu concentrations in primary Osborne ore fluids are typically below 100ppm (Table 4.2; 4.3; Appendix E; F). These are similar to those measured at the Tennant Creek deposits (Zaw et al., 1994) but are lower than measured in ore fluids in other IOCG deposits in the Cloncurry district; at the nearby Starra deposit a maximum Cu concentration of ~2800 ppm was measured in ore stage inclusions with values in primary high salinity fluids typically greater than 1000 ppm (Williams et al., 2001) while average Cu concentrations of 160ppm with a maximum of ~203 ppm are measured at Ernest Henry by PIXE analysis (Mark et al., 1999). PIXE studies of the Starra IOCG deposit in the Cloncurry district examined Cu concentrations in two generations of fluid inclusions. The first, associated with barren magnetite ironstone emplacement at 400-550 ^{o}C, have salinities of 34-52 wt% and Cu concentrations between 190 and 1400 ppm. The second associated with mineralisation hosting hematite deposited at 220-360 ^{o}C have salinities of 29-42 wt% and Cu concentrations of 197 to 2810 ppm (Williams et al., 2001). These concentrations exceed, by up to an order of magnitude, the majority of Cu concentrations measured in pre-mineralisation MS inclusions at Osborne. Therefore the fluid conditions at Osborne must preclude high Cu solubility, leading to saturation at relatively low concentrations. The higher Cu concentrations measured in the fluids at Starra (Williams et al., 2001), are probably a result of the higher fO_2 of the Starra assemblage as indicated by the dominance of hematite in the ironstones and by higher Mn/Fe ratios than at Osborne.

Much higher Cu concentrations, distinctly different from those measured in the IOCG ore fluids, are documented in inclusions from the Lightning Creek magnetite prospect, in the Squirrel Hills Granite (Perring et al., 2000) where ultra high salinity inclusions contain up to 2 wt% Cu. It has been suggested that the granitic intrusions that form the

~1540 Ma Williams and Naraku batholiths may have been a source of ore forming fluids to the IOCG deposits in the region (Perring et al., 2000; Mark et al., 2004; Pollard, 2006). Brine data from the Cloncurry district shows highest Cu concentrations are found in fluids with Br/Cl values that are indicative of a magmatic origin (Williams et al., 1999; Baker et al., 2006; Williams et al., in press) although this data set is potentially skewed by the Lightning Creek data. In most cases the concentration of metals in solution is a function of ligand availability and temperature.

The low Cu concentrations can also provide information on the ore-forming hydrothermal system. In the absence of high Cu concentrations the formation of a >15.2 Mt @ 3.0% Cu system would require a high volume of fluids; assuming an average Cu concentration of 100ppm and near perfect removal of Cu during ore deposition, reducing post-depositional fluid Cu concentrations to 5ppm, then the minimum fluid volume required to form the Osborne deposit would be 1.6×10^{14} litres, or ~1.8×10^{11} tonnes of brine (assuming average fluid density of 1.1g/cm^3). This is approximately half the volume to that estimated to be required to have formed the Mt Isa Cu ore deposit in the Western Fold Belt (Matthäi et al., 2004) and exceeds by an order of magnitude the 4×10^{10} tonnes of fluid that is has been calculated to have formed the Bendigo gold fields (Thompson, 1997).

The volume of fluid that was focused through the Osborne deposit area to form the deposit was 180 km^3. If this fluid volume is assumed to have passed through 1km^2 (approximately the volume of rock that contains the deposit) of the rock then, averaged over 10^6 years, a fluid flux of 5.7×10^{-9} m^3 m^{-2} s^{-1} is calculated. This exceeds the range of fluid fluxes (10^{-10} to 10^{-12}) that are considered typical in metamorphic terranes

(Thompson, 1997). However, this does not take into account the possibility of the shear zones that bound the Osborne deposit, localising and channelling the fluid flow. Time integrated fluid fluxes for pervasive flow through metamorphic terranes are between 10^1 and 10^4 m^3 m^{-2} while in shear zones fluid fluxes are between 10^4 and 10^6 m^3 m^{-2} (Ferry and Dipple, 1991; Ferry, 1994). As discussed in Chapter 2, movement on faults is suggested as having caused the decompression that triggered the massive quartz precipitation or 'silica flooding' (Adshead, 1995). Sibson, (1990), suggested that seismic valving was an important factor in localising flow in faults, and this has been invoked as a mechanism for bringing basinal fluids down into crystalline basement at depths exceeding 10km (Gleeson et al., 2003).

This calculated volume of fluid, 180km^3, that would have passed through the 1km^3 package of rocks that host the Osborne deposit further confirms that fluid-rock ratios were high and that fluid-rock reactions would not have been a significant control on Br/Cl values.

4.4.4 Redox controls

The mineral assemblages in the different domains at Osborne suggest there was a redox gradient across the deposit with ore zones in the western domain hematite bearing and dominated by chalcopyrite with pyrrhotite absent, while pyrrhotite is common component of the pyrite-chalcopyrite sulphide ore assemblage in the eastern domain ore and the deeper parts of the 1SS ore zone. Mn/Fe ratios have commonly been used as a proxy for the redox state of fluids (Bottrell and Yardley, 1991; Yardley et al., 2000) with values below 0.24 associated with fluids equilibrated with pyrrhotite bearing rocks while in fluids equilibrated with hematite-bearing assemblages will have higher Mn/Fe

values. These ratios are a function of the impact of redox conditions on iron solubility; ferrous iron (Fe^{2+}) is much more soluble than ferric iron (Fe^{3+}) so more reduced environments will give rise to fluids with lower Mn/Fe ratios. Bottrell and Yardley, (1991), measured Mn/Fe ratios exceeding 1 in fluids from a hematite-bearing host rock while fluids from a graphitic rock had much lower values. Other factors, besides redox, can also control Mn/Fe values in a fluid, particularly fluid-rock reactions, for example the alteration of albite to biotite which will remove Fe^{2+} from the fluid. Precipitation of the Fe-bearing sulphides, pyrite, pyrrhotite and chalcopyrite, which form the ore mineral assemblage will also remove Fe from the fluids. However, as the MS and CB inclusions are interpreted as being pre-depositional ore fluids, the Mn/Fe values in the fluids will not have been affected by this process.

Both PIXE and LA-ICP-MS data show the same trends in Mn/Fe ratios within MS inclusions. The majority of MS inclusions in samples from the 1S ore zone in the western domain have Mn/Fe values between 0.26 and 0.32, with a small group having values of 0.86, while values for samples from the 3E ore zone in the eastern domain fall between 0.04 and 0.08. Iron concentrations in the two domains also show a marked contrast reaching a maximum of 17 wt% in the 3E ore zone while fluids associated with more oxidised assemblages in the western domain have iron concentrations below 9 wt%. This is consistent with the differing solubilities of ferric and ferrous iron and the Mn/Fe ratios of the MS fluid inclusions can be considered to reflect the redox state of the ore mineral assemblages.

Previous petrographic and textural studies of the Osborne fluid inclusion assemblage identified the later LVD inclusions as having a direct genetic relationship with sulphide

deposition; secondary trails of LVD inclusions radiate from sulphides grains and are interpreted as 'spent' ore fluids (Adshead, 1995; Chapter 2). The observed link between redox state of the MS fluid and of the sulphide assemblage indicates that the MS fluid inclusions are also genetically linked to the ore deposition.

In the LA-ICP-MS data set two fluids are distinguished; one with low Mn/Fe values and one with higher Mn/Fe, potentially indicating one fluid is reduced and while the other is apparently oxidised. The apparently reduced fluid shows correlation between Mn/Fe values and major cation concentrations while the data for the apparently oxidised fluid is more scattered with regard to cation concentrations (Fig 4.8). This scatter of data is interpreted as the result of greater fluid-rock interaction suggesting that the increased Mn/Fe values of the fluids may be a by-product of variable fluid-host rock reactions, i.e. potassic alteration of albitised pegmatites and the creation and destruction of biotite and can not, therefore, be truly a proxy for redox state. Mn/Fe values could also be altered by Fe-sulphide deposition, however the MS inclusions analysed by PIXE and LA-ICP-MS predate sulphide deposition, so this should not be a factor at Osborne.

Further information on the redox state of the ore fluids can be inferred from Ba concentrations in the ore fluids. PIXE and LA-ICP-MS analyses measured concentrations between 500 and 8000 ppm Ba in the majority of inclusions, with a single high measurement of ~1.5 wt%. These values are lower than concentrations of 1-10 wt% Ba measured in Starra ore fluids (Williams et al., 2001) but the low solubility of barite (Blount, 1977) and its absence from the ore mineral assemblage are indicative of either low sulphur content and/or strongly reducing conditions, such that sulphur is present as sulphide. The high pressures and temperatures that existed during Osborne

ore formation might promote Ba solubility (as $BaSO_4$) as will high salinities, such as found in the Osborne ore fluids (Blount, 1977). In solutions with greater than 1 molal NaCl salinities barite solubility increases with increasing temperature without reaching a maximum (Blount, 1977). Extrapolation of the experimental data for barite solubility, from the experimental limits of 300°C and 1400 bars, suggests that under the conditions (~400°C, ~2000 bars) that the Osborne ore was deposited in, up to 0.15 wt% Ba, as $BaSO_4$, could be dissolved in a fluid, considerably less than is measured in many of the high salinity MS inclusions. Therefore fO_2 of the fluid phase must have favoured sulphide stability throughout ore formation. Furthermore the absence of barite daughter minerals in fluid inclusions (Ba is present in daughter minerals only in CO_2-bearing CB inclusions, remaining in the fluid phase in MS inclusions, suggesting it is bound in carbonate phases) suggests that the fluid must have been reduced so that sulphide was the dominant form of sulphur and sulphate can only have been present at low concentrations. Alternately these fluids may have had very low sulphur content with the sulphur in the ore supplied from another source.

4.4.5 Halogen data and fluid sources

MS and CB inclusions in the Osborne deposit show considerable variation in Br/Cl ratios in the MS inclusions. The lowest Br/Cl values of 0.14×10^{-3} are interpreted as the product of evaporite dissolution (e.g. Böhkle and Irwin, 1992a), while the higher values of $>2.5 \times 10^{-3}$ are typical of those previously measured in bittern brines (Hanor, 1994, Kendrick et al., 2002). While some values fall in the field of magmatic compositions, which has been previously cited as evidence of a magmatic or mantle-derived component in the ore fluids (Böhkle and Irwin, 1992b; Johnson et al., 2000; Kendrick et al., 2001), these data can also be produced by mixing between these two

end member compositions, or to be evidence of the variable dissolution of evaporite sequences by circulating bittern brines. The highest Br/Cl values exceed 11.5×10^{-3}, greater than values expected from evaporation of seawater to produce bittern brines (Fontes and Matray, 1993). Although the high uncertainties (up to 50%) in Cl analysis could account for much of the variation, the highest measured Br/Cl values would still exceed 11.5×10^{-3} even allowing for a 50% decrease in measured Cl and so could be considered indicative of genuine fluid processes.

The similar ranges of Br/Cl values measured in both CB and MS inclusions is evidence for acquisition of salinity from multiple sources and also implies that the Br/Cl variation is attributable to processes that occurred before phase separation. Therefore the variation can not be the result of the fluid mixing processes that have been inferred from decreasing salinities and temperatures later in the evolution of the deposit. If the salinity was acquired from sources distal from the Osborne deposit a more homogenous Br/Cl signal would be expected. Therefore the variation in Br/Cl ratios in even the earliest CB inclusions implies that one component of the salinity was acquired locally.

The Osborne deposit has been dated to having formed at 1595 Ma (Gauthier et al., 2001) and mineralisation must have occurred within a few million years of the local peak of metamorphism. Thus the highest Br/Cl values may be the result of metamorphic processes. Zhou and Adshead (1996), suggested that the observed reduction in salinity of the Osborne ore fluids over the depositional history may be the result of uptake of Cl by silicate minerals, including biotite, hornblende and ferropyrosmalite. Uptake of Cl and exclusion of Br in this way could result in relatively increased Br concentrations in the fluid giving rise to elevated Br/Cl values, although

the partitioning of Br in ferropyrosmalite has not been studied. However, studies of halogen ratios in mariolitic scapolite have shown that Br/Cl ratios closely reflect the halogen composition of co-existing fluids and thus uptake of Cl into scapolite would not be expected to affect halogen sequences of hydrothermal fluids (Pan and Dong, 2003).

Biotite is a common mineral at Osborne, occurring as both a primary and secondary phase in the majority of host and metasomatic rock types (Adshead, 1995). Electron microprobe analyses of biotite in pre-ore mineral assemblages and biotite coeval with silica-flooding and ore emplacement show an increase in Cl content from less than 0.3 wt% to as high as 1.2 wt% (Adshead, 1995). If an average uptake of 0.5 wt% Cl is assumed then 5000 ppm Cl would have been lost from the fluid per kg of biotite. The pre-ore deposition fluid can be considered to contain 50 wt% NaCl, equivalent to 30.3 wt% Cl^-. Given a starting Br/Cl composition of 0.5×10^{-3} (Br = 151.5ppm), a simple mass balance calculation shows that driving Br/Cl values to bittern brine-like values of 3.0×10^{-3} would involve a loss of 252500ppm Cl^-, requiring that each litre of ore fluid react to form 50.5 kg biotite, assuming efficient reactions. Given the low Cu content of the fluid and the >15.2 Mt size of the Osborne, a minimum 1.6×10^{14} litres of fluid would have been required to form the deposit (see section 4.4.3) suggestng that the low fluid-rock ratio required to drive Br/Cl changes is unlikely to have been possible, except perhaps near the edges of the fluid channelways. The variation observed in Br/Cl values can therefore be considered to be most consistent with halogens having been derived from different sources of salinity, rather than water-silicate interaction.

A number of studies have examined the exchange of Cl between saline fluids and minerals including biotite, scapolite, apatite and amphiboles (Mora and Valley, 1989;

Kullerud, 1996; Markl et al., 1998; Kullerud and Erambert, 1999; Pan and Dong, 2003). Cl is strongly partitioned into the aqueous phase and will be removed from the solid phase by metamorphic devolatilisation and infiltration of dilute fluids (Mora and Valley, 1989), and the incorporation of Cl into silicate minerals can be used as an indicator of the activity of Cl (Kullerud, 1996; Kullerud and Erambert, 1999). Kullerud (1996) has demonstrated that the Cl content of amphibole is controlled principally by the activity ratio a_{Cl}^-/a_{OH}^- of the fluid with which it equilibrated. Cl substitution into amphibole, biotite and ferropyrosmalite, as recognised by Zhou and Adshead, (1996) at Osborne, is an exchange reaction, which is controlled by similar equilibria. This suggests Cl will only substitute into the silicate minerals when a_{Cl}^-/a_{OH}^- is high; i.e. at high salinities. A reduction in salinity would result in a decrease of X_{Cl} in amphiboles and biotites (Mora and Valley, 1989). Other studies contend that the enrichment of Cl^- in biotites is controlled by $f(HCl)/f(H_2O)$, and not by the salinity of the fluid and $f(HCl)/f(H_2O)$ will be low where there is high fluid flux (Munoz and Swenson, 1981). Rubenach, (2005b), examined chlorine enriched biotite spatially associated with zones of albitisation in the Snake Creek anticline, to the north of Osborne in the Eastern Fold Belt, and concluded that the Cl enrichment occurred in the waning stages of albitisation, as fluid flux decreased and $f(HCl)/f(H_2O)$ increased.

Therefore, the high Cl content measured in hornblende, biotite and ferropyrosmalite at Osborne (Zhou and Adshead, 1996; Adshead et al., 1998) can be considered a product of equilibrium with the high salinity fluids, as trapped within MS inclusions. Uptake of Cl^- by these minerals in most likely to have occurred as fluid fluxes declined, which would be expected towards the end of ore formation. Both mass balance calculations and studies of Cl^- uptake by silicate minerals suggest the observed decrease in salinity

during ore formation at Osborne can be attributed to fluid mixing processes during ore formation and not removal of Cl^- from the fluid by fluid-rock reactions.

Previous PIXE data for Osborne did not show such a spread of data as is identified in this study, with bittern brine-like compositions not identified (Williams et al., in press), but the range of values measured in this study fits with the variation observed by using combined noble gas and halogen analysis (Fig 4.11). More extreme values are observed using PIXE but this is to be expected as the method measures individual inclusions while combined noble gas and halogen analysis is a semi-selective bulk technique which will homogenise more extreme values. There is also greater uncertainty in the ratios due to the large errors (<50%) in the measurement of Cl (Ryan et al., 1995), although it can be constrained with better certainty from microthermometric salinity estimates (see Chapter 2).

Fluids associated with the 1S and 1SS ore zones have Br concentrations a magnitude greater than in the eastern domain and pegmatite fluids (Appendix E). These high Br concentrations correlate with highest Br/Cl values. As the development of the most extreme Br/Cl values by loss of Cl through fluid-rock interaction is unlikely, this distinction in Br concentrations between the different ore zones can be taken as further evidence for multiple fluid sources.

4.4.6 Reconstruction of a typical fluid inclusion composition

When a basic charge balance of major cations (measured by PIXE) against chlorine is carried out to estimate Na contents, some of the inclusions do not have enough Cl^- to balance the measured cations, while others have excess, which is to be expected given

the errors incurred. As Cl analyses by PIXE are extremely depth sensitive and may incur errors of up to 50%, reconstructions of a typical fluid inclusion composition must be carried out with care. To reconstruct the composition of pre-deposition ore fluids (such as those entrapped within MS inclusions) the measured compositions of inclusions analysed by both LA-ICP-MS and PIXE are examined.

Element	Concentration (ppm)	
	37B_1_11 (CB)	***852_1_6 (MS)***
Na^{+}	104200	130380
K^{+}	54090	40320
Ca^{2+}	24890	12460
Mn^{2+}	6310	13030
Fe^{2+}	87230	54220
Cu^{+}	40	40
Zn^{2+}	760	8000
As^{3+}	140	640
Rb^{+}	330	430
Sr^{2+}	330	150
Ba^{2+}	1770	510
Pb^{2+}	150	2390
Br^{-} ^	480	440
Cl^{-} *	401970	354770

Table 4.7: Reconstructed representation of fluid compositions from ore stage and pegmatite sample inclusions.
Cation data is taken from laser ablation data sets,
**Cl content is calculated using Fe/Cl ratio in PIXE data, and Fe concentration measured by laser ablation*
^ Br concentration is calculated from PIXE Br/Cl ratio and estimated Cl concentration.

In the element ratio comparisons of fluid inclusion compositions analysed by both PIXE and LA-ICP-MS inclusions 37B_1_11 and 852_1_6 show the greatest similarities. As PIXE analyses of concentrations incur up to 30% errors the concentrations measured by LA-ICP-MS are taken for all elements except Cl and Br. Cl^{-} concentrations are estimated by performing a simple charge balance for the measured cation concentrations. Br is calculated from PIXE Br/Fe ratios. Cl PIXE data, and Br/Cl ratios are not used due to the higher uncertainties associated with the measurement of Cl.

Br/Fe was chosen as Fe shows most consistency when ratioed with other elements (see Fig 4.4). Br/Cl values generated by these calculations are within the ranges measured by PIXE and noble gas analyses in these samples. Example concentrations are given for an ore stage sample (37B_1_11) and a pegmatite sample (852_1_6; Table 4.7).

4.5 Conclusions

The Osborne ore fluids had very high salinities (of 50-70 wt% salts) and dissolved metal contents (<17 wt% Fe), similar to those documented in magmatic fluids. However, this similarity is attributed to comparable pressure and temperature conditions, rather than a implying that the Osborne fluids were magmatic.

Very high Fe contents, particularly in the 3E ore samples, and low Mn/Fe ratios are interpreted to reflect a reducing environment. The presence in the 3E ore lens of CH_4 in the vapour phase of fluid inclusions and of pyrrhotite in the ore assemblage supports this interpretation and also confirms a link between the primary CB and MS ore fluids and ore deposition.

MS and CB inclusions exhibit no systematic differences in composition and the MS inclusions can therefore be considered to have entrapped the unmixed brine portion of CB inclusions. Both inclusion types have very varied Br/Cl values, similar to those measured by combined noble gas and halogen analysis, although PIXE analysis measures more extreme values. The range of values supports multiple sources of salinity. Development of the observed variation in Br/Cl by fractionation caused by uptake of Cl by silicate minerals during fluid rock reaction is unlikely given the high salinity of the fluids.

Lowest Br/Cl values are indicative of an evaporitic source for salinity. This is also supported by high Na/K values. An order of magnitude difference in Br concentrations measured in fluids in the eastern and western domain ore samples also supports multiple sources of salinity, and fluid mixing. However, the concentrations of less conservative elements, particularly the major cations, Na, K and Ca, are considered to be influenced by the fluid-rock reactions which generated the hydrothermal alteration assemblage.

High concentrations of Ba limit the amount of dissolved sulphate than can have been transported in the fluid and may suggest that a second fluid must have transported sulphur. Alternately, strongly reducing conditions can be inferred from the presence of dissolved Ba and absence of barite in the ore mineral assemblage. This is also implied by the presence of pyrrhotite and low Mn/Fe values in the 3E ore zone. Barium may, therefore, have been transported complexed by Cl^- in a sulphide bearing fluid. In a single fluid model the amount of sulphur transported by the ore fluid would be controlled by the solubility of the sulphide ore minerals.

The ore fluids were undersaturated with respect to Cu at 600^{o}C. Cooling is implicated as a deposition mechanism although changes in fluid pH and redox state caused by fluid mixing may also have been significant. These conclusions are supported by the microthermometry and halogen data which indicates fluid cooling and mixing during formation of the Osborne deposit.

5. GEOCHEMICAL INTERPRETATION AND MODELLING OF THE FORMATION OF THE OSBORNE IOCG DEPOSIT

5.1 Introduction

This study of the fluid inclusion assemblage hosted by the ore stage mineral assemblage at Osborne has identified several generations of fluids associated with silica flooding, Cu-Au deposition and post-mineralisation fluid flow. In previous chapters microanalysis of these fluid inclusion populations has identified the conditions under which the ore fluids were trapped and evidence for fluid unmixing and mixing (Chapter 2). The source of the fluids, and how they acquired their high salinity was discussed (Chapter 3; Chapter 4) and an average composition was determined for the brine component of early high salinity, CO_2-bearing ore fluid (Chapter 4).

The earliest generation of ore-forming fluid was trapped as CB-type inclusions; a high salinity fluid with $XCO_2 \approx 0.15$ that underwent phase separation forming a ultra-high salinity brine and separate CO_2 fluid that were trapped in MS- and CO_2-type inclusions. The MS inclusions contain chemically complex brines with measured salinities exceeding 47 wt% NaCl equivalent. LVD inclusions occur in trails that radiate from sulphide grains and are thought to have entrapped 'spent' post-deposition ore fluids with salinities between 17 and 38 wt% NaCl equivalent.

Examination of halogen data from PIXE and combined noble gas and halogen analysis shows considerable variation in Br/Cl and I/Cl values measured in MS and LVD inclusions. The range of values is interpreted as evidence for multiple sources

of salinity with low Br/Cl values of ~0.2 × 10^{-3} considered to be derived from the dissolution of evaporites (Böhkle and Irwin, 1992a: Chapter 3: Chapter 4) while higher Br/Cl values of <2 × 10^{-3} are considered to be bittern brine-like fluids or the product of metamorphic dewatering and volatile release (Chapter 3; Kendrick et al., 2006b; Kendrick et al, 2007b). A full range of values are measured from one end member composition to the other, which is indicative of fluid mixing.

Invoking fluid mixing at the Osborne deposit raises a number of questions with respect to ore genesis: Was fluid mixing the trigger for ore deposition? Does the variation in Cu:Au and redox state across the deposit imply that Cu and Au were transported by different fluids? And if so, which fluid transported which metal? Geochemical modelling in this chapter attempts to evaluate some of these questions.

5.2 Solubility of Cu, Au, Fe and Si, and ore formation

The solubility of many metals in solution is enhanced by their interaction with anions (or ligands) to form complexes. Many transition metals form chloride complexes in solution, including Fe, Cu, Pb and Zn. Chloride complexes are the most important for metal transport in hydrothermal solutions, particularly given the dominance of the Cl^- anion within such fluids. Metals are scavenged from source rocks or magmas and transported by these complexes (Helgeson et al., 1981). With increasing chloride concentrations, complexes will form with greater numbers of Cl^- per metal ion. However complex geometry has also been shown to have an influence, making some complexes with less Cl^- ions more stable than others with greater numbers of Cl^- ions (Henley, 1984).

The formation of copper chloride complexes controls the solubility of copper oxide and sulphide minerals in hydrothermal fluids. As Cu and Fe chloride complexes form in solutions with high chloride concentration the solubility of chalcopyrite will increase with increasing temperature under constant pressure conditions. The inverse relationship is observed in more dilute fluids in which Cu^{+} and Fe^{2+} predominate over $CuCl_3^{2-}$ and $FeCl_2^{0}$, suggesting fluid dilution can drive precipitation of chalcopyrite (Helgeson, 1992).

In studies of copper chloride complexes at high temperatures the formation of CuCl, $CuCl_2^{-}$, $CuCl_3^{2-}$ and $CuCl_4^{3-}$ have been inferred from solubility measurements and optical spectra (e.g. Liu et al., 2002; Liu and McPhail, 2005). However, it has been noted that no other monovalent cations form tri- and tetra-chloro complexes which suggests that at high temperatures $CuCl_2^{-}$ will be the dominant complex in hydrothermal brines (Sherman, 2007). This is supported by XAFS spectra of high temperature Cu-Cl solutions which show only CuCl and $CuCl_2^{-}$ above 100^{o}C (Fulton et al., 2000). In studies of Fe solubility in hydrothermal fluids and the formation of FeCl complexes, both $FeCl^{+}$ and $FeCl_2^{0}$ have been shown to be significant (Crerar et al., 1978). Experimental data for supercritical fluids show that at higher temperatures $FeCl_2^{0}$ becomes dominant and is the main control on Fe solubility (Fein et al., 1992).

Temperature has been found to be the major factor controlling chalcopyrite solubility and precipitation (Hezarkhani et al., 1999; Ulrich et al., 2001; Liu and McPhail, 2005). At pressures of 1kbar, a decrease in temperature from 500 to 300^{o}C in a 10 molal chloride solution will decrease chalcopyrite solubility from 273ppm to 1ppm in solutions buffered by a hematite-magnetite-pyrite assemblage and from 128ppm to

0.5ppm in magnetite-pyrite-pyrrhotite buffered solutions (Liu and McPhail, 2005). This data also demonstrates the control of redox on chalcopyrite solubilities, with increased solubility of chalcopyrite associated with more oxidised fluids. Seyfried and Ding, (1993) found that Cu concentrations decreased and Fe concentrations increased with decreasing fO_2. Studies suggest decreased pressure will result in higher chalcopyrite solubility (Hemley et al., 1992; Liu and McPhail, 2005).

Processes such as fluid mixing and fluid rock reactions will change the physiochemical conditions of the fluids, precipitating chalcopyrite (Woitsekhowskaya and Hemley, 1995; Liu and McPhail, 2005). Fluid mixing can result in changes to Cl^- concentrations and pH. Decreases in f_{O_2} and Cl^- concentrations will reduce Cu solubility while in a 10 molal NaCl solution an increase from pH 4 to pH 6 would decrease Cu concentrations by over an order of magnitude (Liu and McPhail, 2005). However, a study of synthetic fluid inclusions indicated that mixing processes are not significant above 500 ^oC where high temperatures are the dominant control on Cu solubility (Hack and Mavrogenes, 2006). Further discussion of the controls on copper solubility can be found in Chapter 4.

Data for the solubility of gold complexes in the temperature range of ore formation at Osborne is limited. An experimental study of gold solubility in NaCl- and H_2S-bearing fluids at temperatures of 250 to 350^oC showed that gold solubility is independent of aCl^- and pH, suggesting that chloride complexes are not important in the hydrothermal transport of gold under reducing conditions (Hayashi and Ohmoto, 1991) although Cl-complexed Au is potentially significant in oxidised fluids and at

higher temperatures. The high salinity of the Osborne ore fluids would also promote the formation of Au-chloride complexes.

Gold solubility was shown to increase with increased $H_2S_{(aq)}$ activity indicating the main complexes involved in transport of gold under reducing conditions are bisulphide complexes (Hayashi and Ohmoto, 1991). Thus, for there to be gold mobility the fluid must contain sulphur, and the redox state and pH of the fluid must be such that sulphur is present as sulphide. Three main bisulphide complexes have been identified: $Au(HS)^0$; $Au(HS)_2^-$; $Au_2(HS)_2S^{2-}$ (Henley, 1984):

$$Au + H_2S^0 = Au(HS)^0 + 0.5H_2 \quad (5.1)$$

$$Au + H_2S^0 + HS^- = Au(HS)_2^- + 0.5H_2 \quad (5.2)$$

$$2Au + 2HS^- + 2H^+ + S^{2-} = Au_2(HS)_2S^{2-} + 0.5H_2 \quad (5.3)$$

Hayashi and Ohmoto, (1991), found that gold predominately formed bisulphide complexes according to the reaction:

$$Au_{(s)} + 2H_2S_{(aq)} \leftrightarrow HAu(HS)_2^0 + ½H_{2(aq)} \quad (5.4)$$

The dissolution of gold to form these complexes liberates hydrogen, therefore, under strongly reducing conditions gold solubility will be lowered (Henley, 1984). However, if the fluid is oxidised so that sulphate becomes the dominant complex gold solubility will also decrease (Seward, 1973). pH is also significant; reaction 5.2 above involves both H_2S and HS^- species so maximum gold solubility will be achieved at a pH close to the boundary between the predominance fields for these two

complexes, and solubility will decrease with increasing and decreasing pH (Henley, 1984).

Benning and Seward examined the solubility of gold in hydrothermal solutions at temperatures of 150-400^{o}C and between 500-1500 bars. Experiments were run with varying pH and total reduced sulphur concentrations. They found high gold solubilities of 2-108 ppm occurred in fluids with high total reduced sulphur and near neutral pH while lowest solubilities were found in fluids with low total reduced sulphur and acidic pH. The solubility maximum at near neutral pH was attributed to the formation of $Au(HS)_2^-$ (see equation 5.2 above). However, at higher temperatures the maximum solubility shifts to higher pH values and $AuHS^0$ becomes the most significant complex for gold transport (Benning and Seward, 1996).

The deposition of gold at the Osborne deposit would therefore be favoured by a shift in chemical conditions, changing redox and pH conditions. Cu:Au ratios at Osborne vary widely across the deposit which could be interpreted as evidence for transport of two metals in different fluids. Mixing between the two fluids would cause the necessary perturbations in pH and redox, resulting in ore deposition. Increased activity of $H_{2(aq)}$ by reaction with ferrous iron-bearing minerals, or decreased activity of $H_2S_{(aq)}$ by precipitation of sulphide minerals are invoked as mechanisms for gold deposition (Hayashi and Ohmoto, 1991).

The solubility of quartz must also be considered when discussing the deposition of the Osborne ore, as the Cu-Au mineralisation is hosted by extensive hydrothermal quartz ('silica flooding'). The effects of a rapid, large decrease in pressure on silica

solubility were discussed in Chapter 2. Smaller shifts in pressure are less significant than changes in temperature (Fournier and Potter, 1982). pH also exerts a control on silica solubility with higher pH promoting dissolution of quartz (Fleming and Crerar, 1982), however this effect is only significant above pH values of 8, which are much higher than would be expected in most hydrothermal fluids (Rimstidt, 1997). Increasing silica solubility is also observed as a result of increased fluid salinity; at elevated pressures this salting-in effect (Xie and Walther, 1993) is only observed at high temperatures and the reverse effect is observed at lower temperatures. At 1 kbar in a 4 molal NaCl solution a salting out of silica is observed below 400^{o}C and salting in occurs only above 400^{o}C (Xie and Walther, 1993).

The main mechanisms invoked for ore deposition from Au, Cu and Fe bearing brines are decreases in temperature, dilution of chloride concentrations and changes to fluid pH and redox (Crerar et al., 1978; Henley, 1984; Hayashi and Ohmoto, 1991; Liu and McPhail, 2005). Changes in pressure, pH and temperature will also change silica solubility. In addition metals such as Cu and Fe that are transported as chloride complexes and are precipitated as sulphides will become saturated as reduced sulphur content increases, i.e. by fluid mixing or reaction with sulphide-bearing rocks.

Decreases in temperature are documented in the fluid inclusion assemblage at Osborne, as is an apparent dilution (Chapter 2). Both fluid dilution and fluid-rock reactions will change the fluid pH and redox state. Therefore for the purposes of modelling ore-forming processes at Osborne both cooling and dilution will be examined.

Fluid compositions to be used for modelling can in most part be deduced from fluid inclusion analysis (see Chapter 4). However, studies of these inclusions do not measure quantifiable sulphur or gold. Concentrations of gold required to form a deposit, estimated from fluid inclusion studies, are between 1 and 100 ppb (Seward and Barnes, 1997), while experimental data from synthetic fluid inclusions suggest that at 600^{o}C and pressures of 2-4kbar, Au concentrations can reach ~1000ppm (Loucks and Mavrogenes, 1999).

5.3 Geochemical modelling

In previous chapters the composition of the ore-bearing fluids has been defined and both pre-deposition and post-deposition fluid inclusion populations identified. In order to investigate some the questions raised by the geochemical analyses and define the extent and importance of fluid-rock interactions and fluid-mixing processes in the genesis of the Osborne deposit, the HCh modeling program (Sharov and Bastrokov, 1999) has been used to examine a number of scenarios and produce geochemical models.

HCh models are based upon 'step-flow-through-reactor' style modelling (Cleverley and Oliver, 2005). Each equilibrium calculation for a given set of conditions is termed a step (i). A series of steps for the same calculation are termed a step series (Fig. 5.1A;B). Step series can also be modelled with changes in the equilibrium calculation: each step series within these multiple step series models are termed waves (N) (Fig. 5.1C;D). The thermodynamic data used for this study are based on the Geoscience Australia version of the UNITHERM database (Bastrokov, 2003) with additional data from the ETH version of SUPCRT (Pokrovskii et al., 1998) and Fe

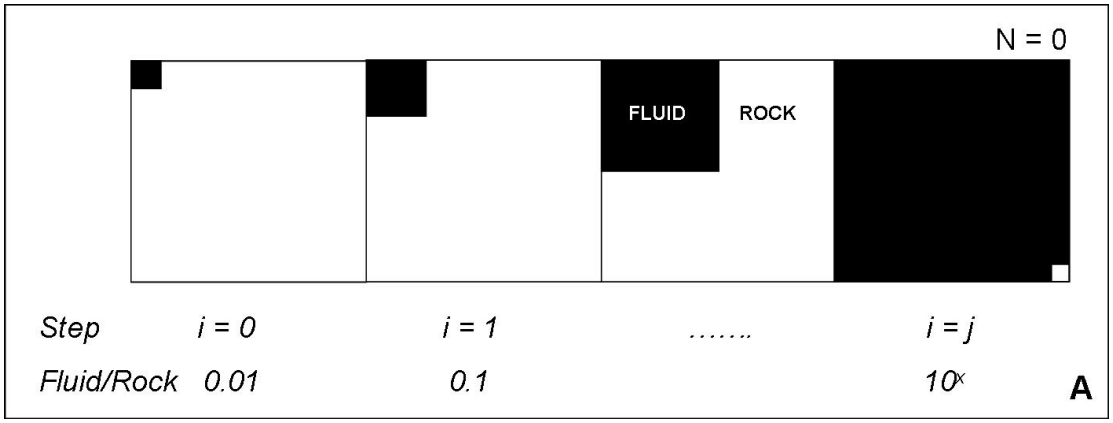
N = 0
FLUID
ROCK
Step
i = 0
i = 1
…….
i = j
Fluid/Rock
0.01
0.1
10x
A

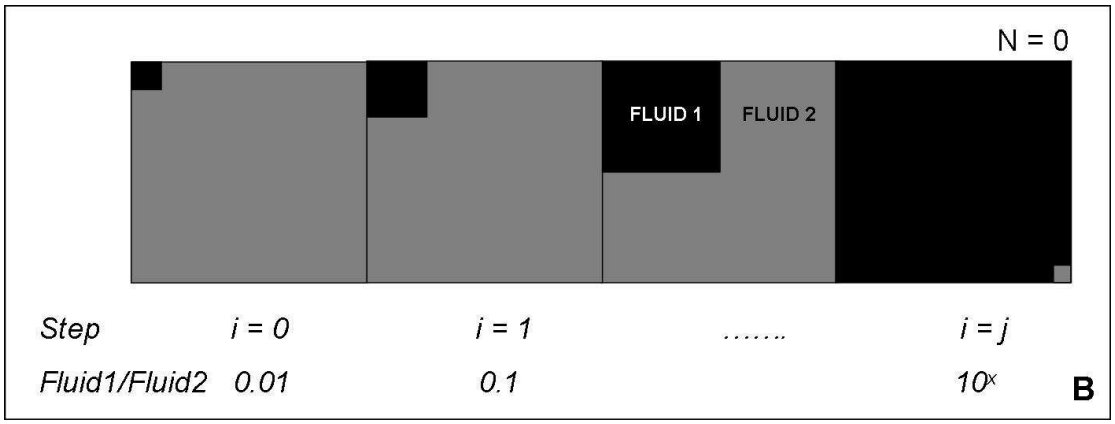
N = 0
FLUID 1
FLUID 2
Step
i = 0
i = 1
…….
i = j
Fluid1/Fluid2
0.01
0.1
10x
B

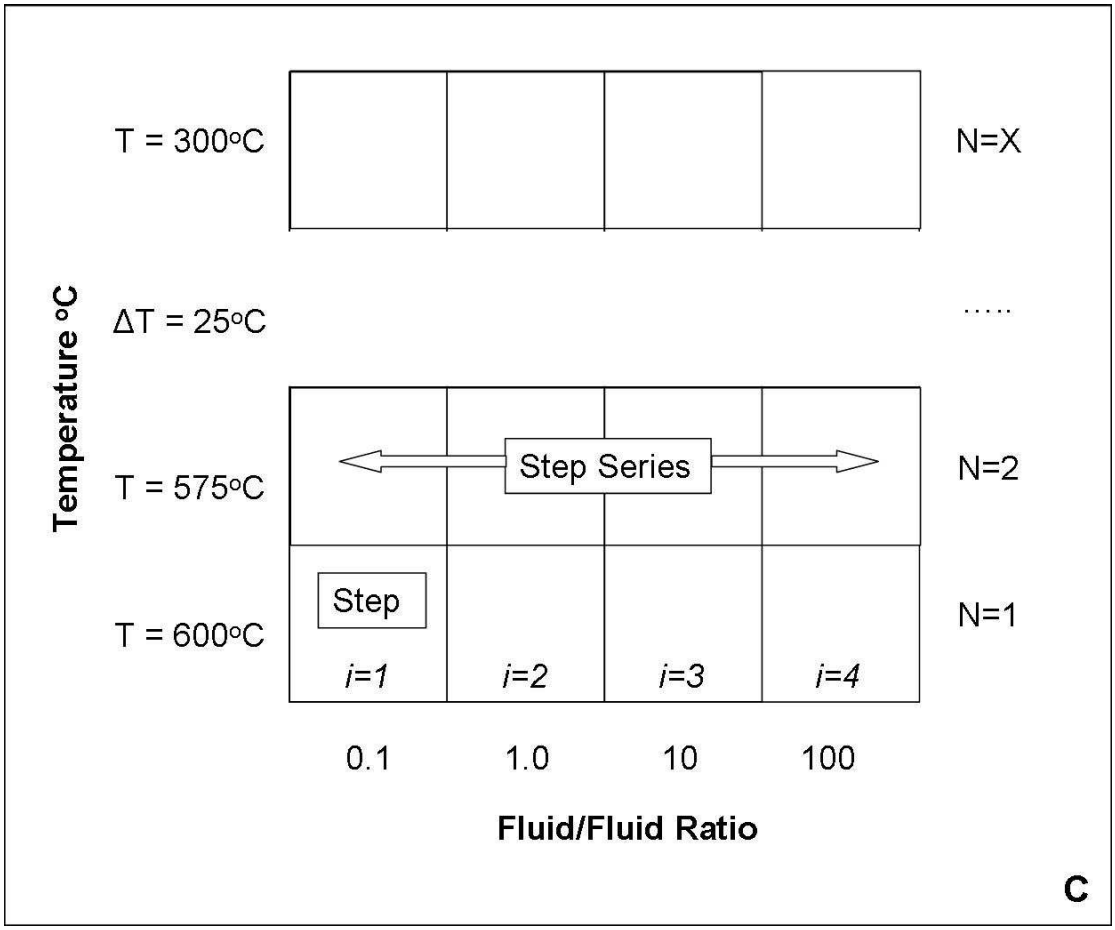
T = 300oC
N=X
ΔT = 25oC
…..
Temperature °C
T = 575oC
Step Series
N=2
T = 600oC
Step
N=1
i=1
i=2
i=3
i=4
0.1
1.0
10
100
Fluid/Fluid Ratio
C

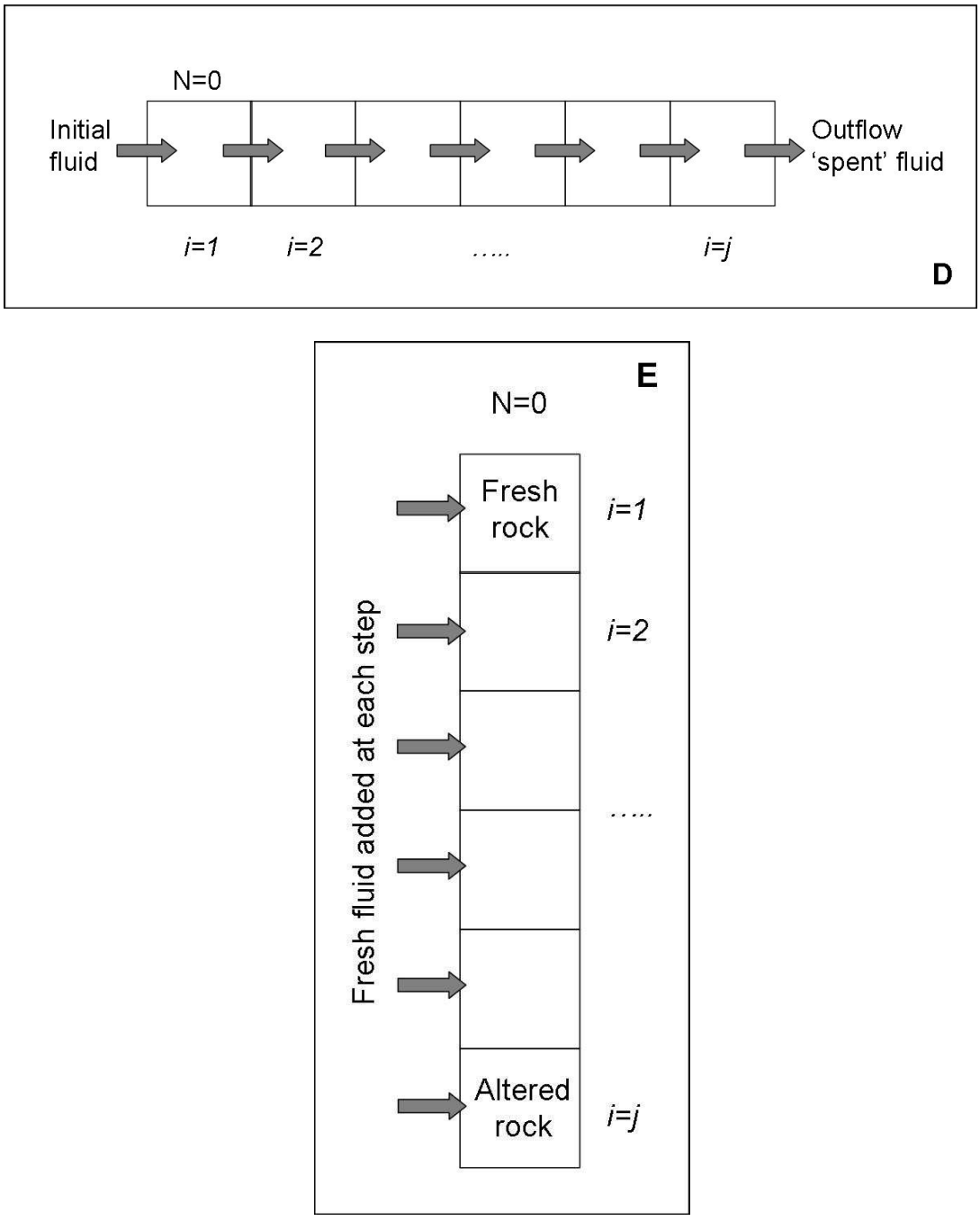

Figure 5.1: Box diagrams for different modeling methodologies used to test hypotheses for the genesis of the Osborne deposit, (after Cleverley and Oliver., 2005).
(A) Single Step Series, Batch reaction model for variable fluid-rock ratios.
(B) Single Step Series, Batch reaction model for variable fluid proportions during fluid mixing
These single step series are titration models in which increasing amounts of fluid are added to rock/a second fluid with each step.
(C) Multiple Step Series, Batch reaction model for variable fluid mixing ratios and temperatures. In this model one fluid is titrated by another. Each step has a different fluid:fluid ratio and the step series can be combined with step series from other waves to examine the effects of changing temperature.
(D) Fluid flow through model. In this model the composition of the fluid that has reacted with rock in the previous step is carried through to react with fresh rock in the next step. Such a model could be used to examine redox boundaries.
(E) Flush model. In this model the composition of the rock from the previous step that has reacted with fluid is carried through to the next step and reacted with fresh fluid. Such a model will predict alteration assemblages at different fluid:rock ratios.

and Cu complexes from Shock et al., (1997) and Sverjensky et al., (1997). This is the same data set as used by Cleverley and Oliver (2005) to model potassic alteration at Ernest Henry.

Two main types of models have been carried out; (1) batch process models, used to identify the main reactions taking place in a static state system, in which each step is a separate reaction with no connection to other steps (Fig. 5.1A;B;C) and which can be modelled at different PTx conditions, and (2) fluid flow-through models in which the composition of the reacted fluid is carried through to the next step of the model allowing the evolution of the fluid to be tracked (Fig. 5.1D) or flush models in which the composition of the solid phase is carried through to the next step of the model with fresh fluid added each time (Fig. 5.1E). The main fluid composition used in the models is a high salinity, CO_2- and sulphur-bearing brine with chemistry analogous to that measured in CB inclusions (Table 5.1; Section 4.4.7), although for the purposes of modelling the concentrations have been diluted by a factor of three (see section 5.3.1) and sulphur concentrations are modified for each model (further detail given in model descriptions).

5.3.1 Geochemical modelling considerations

Hydrothermal systems in nature are inherently complex, with fluid flow varying in three dimensions and time. Therefore modelling an ore forming system requires simplification of the fluid and rock chemistry to permit the model to run within the confines of the modelling program (Heinrich et al., 1996). This simplification needs to be done carefully so that the model still produces geologically realistic information.

Due to extremely limited data describing the thermodynamic behaviour of high salinity fluids at the temperature and pressure conditions documented at Osborne and the subsequent limitations of the HCh modelling software, for the purpose of this exercise the composition of the high salinity ore forming fluid that is input into the models has been diluted by a factor of three. An examination of metalliferous brine compositions with varied (basinal, metamorphic and magmatic) origins and from environments with a broad range of pressure and temperature conditions, compiled by Yardley, (2005), show that the overall metal content of a fluid is a function of chloride content, and metal ratios are more strongly controlled by temperature. Therefore the dilution of the fluids for modelling will allow the processes of ore formation to be modelled, but there will not be a correct mass-balance. It must also be considered that relationships between chalcopyrite solubility, fluid salinity and other factors such as activity coefficients are unlikely to be linear at the ultra-high salinities found in the MS inclusions and so any comparison of the modelling results presented in this chapter with mineralogy and grade zonation at Osborne is necessarily limited.

Heinrich et al., (1996) note that the thermodynamic behaviour of iron often plays a key role in ore-forming systems, requiring Fe-Mg and Fe-Al silicate solid-solutions to be considered in models in order to better constrain cation exchange and redox reactions. Therefore, for this study, biotite is modelled in HCh as a solid solution. Plagioclase is also modelled as a solid solution to enable cation exchange between fluid and rock to be examined.

The data used for fluid compositions is derived from PIXE and LA-ICP-MS data and thus must be considered to incur the <30% errors associated with these methods. The rock compositions are derived from XRF analyses and so can be considered more accurate. The HCh program assumes that the chemical equilibrium is achieved at each step. Where fluid rock is through a network of pores then equilibrium is likely to be reached. However, where fluid flow is through a fracture network or shears, as was probably the case at Osborne (see Chapter 4), equilibrium is less likely to have been reached and so the results of the modelling must be interpreted with consideration of this limitation.

5.3.2 Static closed system batch process models

These batch process models have no mass-transfer between steps. Each step is a separate equilibrium calculation. These models have been used to test the importance of different degrees of fluid:rock ratios and fluid proportions in fluid mixing.

In order to test the significance of the different host rock types in determining the redox state of the ore mineral assemblages fluid-rock reactions have been modelled using rock compositions from the Western and Eastern domains (analysed by XRF; Adshead, 1995). The composition data used for the models are given in Table 5.1. The numerical algorithms used for the control files of each model type are based on those specified by Cleverley and Oliver (2005) in a study of potassic alteration at the Ernest Henry IOCG deposit (Appendix G).

The initial phase of modelling required an understanding of how much sulphur the ore fluids would have to contain to precipitate the Osborne ore minerals. Using HCh and

	[1] Eastern Domain rock	[2] CB fluid	[3] Western Domain rock	[4] Mixing fluid
H_20	5×10^{-4} kg	1.0 kg	5×10^{-4} kg	1.0 kg
NaCl	0	2.3 mol	0	1.0 mol
KCl	0	9.2×10^{-1} mol	0	1.0×10^{-1} mol
$CaCl_2$	0	4.3×10^{-1} mol	0	9.0×10^{-1} mol
$FeCl_2$	0	1.3 mol	0	2.1×10^{-1} mol
$MnCl_2$	0	1.0×10^{-1} mol	0	5.0×10^{-4} mol
CuCl	0	5.0×10^{-4} mol	0	5.0×10^{-6} mol
$ZnCl_2$	0	1.1×10^{-3} mol	0	1.0×10^{-6} mol
$PbCl_2$	0	1.0×10^{-3} mol	0	1.0×10^{-6} mol
H_2CO_3	0	2.0×10^{-1} mol	0	5.0×10^{-3} mol
CH_4	0	1.0×10^{-3} mol	0	2.0 mol*
N_2	0	1.0×10^{-2} mol	0	0
H_2S	0	0.5×10^{-4} mol*	0	2.0 mol*
HSO_4	0	0.5×10^{-2} mol*	0	5.4×10^{-4} mol*
SiO_2	5.6×10^{-1} kg	0	7.5×10^{-1} kg	0
TiO_2	3.1×10^{-3} kg	0	1.0×10^{-4} kg	0
Al_2O_3	2.2×10^{-1} kg	0	7.0×10^{-3} kg	0
Fe_3O_4	1.2×10^{-1} kg	0	2.0×10^{-1} kg	0
MnO	2.0×10^{-4} kg	0	1.0×10^{-4} kg	0
MgO	5.3×10^{-3} kg	0	2.0×10^{-3} kg	0
CaO	7.2×10^{-3} kg	0	2.2×10^{-3} kg	0
Na_2O	6.0×10^{-2} kg	0	3.2×10^{-2} kg	0
K_2O	3.5×10^{-3} kg	0	1.8×10^{-3} kg	0

Table 5.1: Fluid and rock compositions used in models.
The Western and Eastern domain rock compositions are derived by averaging XRF analyses (Adshead, 1995) and the CB fluid composition is based upon PIXE and LA-ICP-MS analyses (see Chapter 4) with the metal content of the analyses assumed to be paired with Cl so as to achieve a charge balance. Errors can be assumed to similar to those incurred by PIXE analysis: <30% (see discussion in text).
**As these components have not been quantifiably measured each was varied for different models to test what concentrations may have been required for ore formation (see text for details).*

	400°C	**600°C**
H_2S saturation limit	0.0371 moles	1.784 moles
pH	4.4	2.8
Log fO_2	-19.03	-25.76

Table 5.2: Sulphide saturation limits in the dilute CB-type fluid at 400°C and 2000 bars and 600°C and 3000 bars (fluid contains ~25 wt% salts).

the Unitherm database, equilibrium models show that a CB-type fluid (diluted by a factor of three) under the conditions recorded by fluid inclusions and mineral assemblages (600 ^{o}C, 3000 bars) is capable of carrying almost 2 moles of sulphur in solution before sulphide minerals become saturated (Table 5.2). Thus, the (dilute) fluids would need to contain a minimum of 2 moles of reduced sulphur (H_2S) per kg of CB-type fluid before sulphides would be precipitated and the actual CB fluids would require much higher concentrations (~10 moles assuming linear relationships). However, temperatures recorded in fluid inclusions interpreted as being associated with sulphide deposition are between 200 and 400^{o}C (Chapter 2). At 400^{o}C and 2000 bars the amount of H_2S that can be dissolved in the CB-type fluid without precipitating sulphides is less than 5×10^{-2} moles (Table 5.2). As the high Ba content of the fluids indicates that sulphur could not have been transported as sulphate (Chapter 4) the low solubility of sulphur in the fluid suggests that for enough sulphur to be transported to the site of the ore deposit mixing with a second sulphur-bearing fluid must be considered. Alternately, mixing with a second, cooler fluid could have lowered the CB-type fluid temperature causing the ore minerals to become saturated. These scenarios are tested in the HCh modelling detailed below.

The oxidation state of the ore mineral assemblages varies across the Osborne deposit. Magnetite-pyrite-chalcopyrite assemblages are observed in the western domain and pyrrhotite-bearing assemblages in the eastern domain. Large gradients in oxygen fugacity are reported as a feature of interbedded sedimentary rocks that have been metamorphosed to amphibolite facies with the variation in redox interpreted as a result of oxygen being immobile and inert during regional metamorphism, preserving the Fe^{2+}/Fe^{3+} ratios of the sedimentary protoliths (Chinner, 1960; Rumble, 1973).

However, the redox gradients at Osborne can also be linked to changes in Cu:Au values across the deposit which suggests the variation in both redox and Cu:Au may be attributed to variable mixing between two fluids, one Cu-bearing, the other carrying Au.

At Osborne the more reduced, pyrrhotite-rich, ore assemblages are found in the Eastern domain, hosted by schists and pegmatites while the more oxidized assemblages are associated with the banded ironstones of the Western domain. It has been suggested that the redox state of the ore assemblages could be linked to the host rock composition as different mineral assemblages are associated with different host rock types (see Chapter 1). Initial testing of this hypothesis has been carried out for a one fluid model, in which all ore components are transported within a single fluid. Under these conditions if the ore fluids had carried reduced sulphur, as $H_2S_{(aq)}$, the ore metals would be less likely to have been transported without the precipitation of sulphide minerals so reduction of a SO_4^{2-} carrying fluid at the site of mineralisation is proposed. Reaction with the host-rocks is a potential mechanism of reduction. However, when a variable fluid-rock ratio batch reaction model (Fig. 5.1A) is run testing the results of fluid-rock interaction with increasing volumes of fluids, the results show that the host-rocks at Osborne would not reduce a 2 molal SO_4^{2-} fluid, particularly at high fluid-rock ratios (Fig. 5.2; 5.3). Geochemical modelling in HCh suggests that the Eastern and Western domain rocks would have very similar impacts on fluids (Fig. 5.2; 5.3) so the redox gradient observed at Osborne is inconsistent with a host-rock control, and may indicate that the redox state of the mineral assemblage redox is primarily controlled by the composition of the fluids. These findings are consistent with the high Ba content of the fluids measured in the Osborne fluids

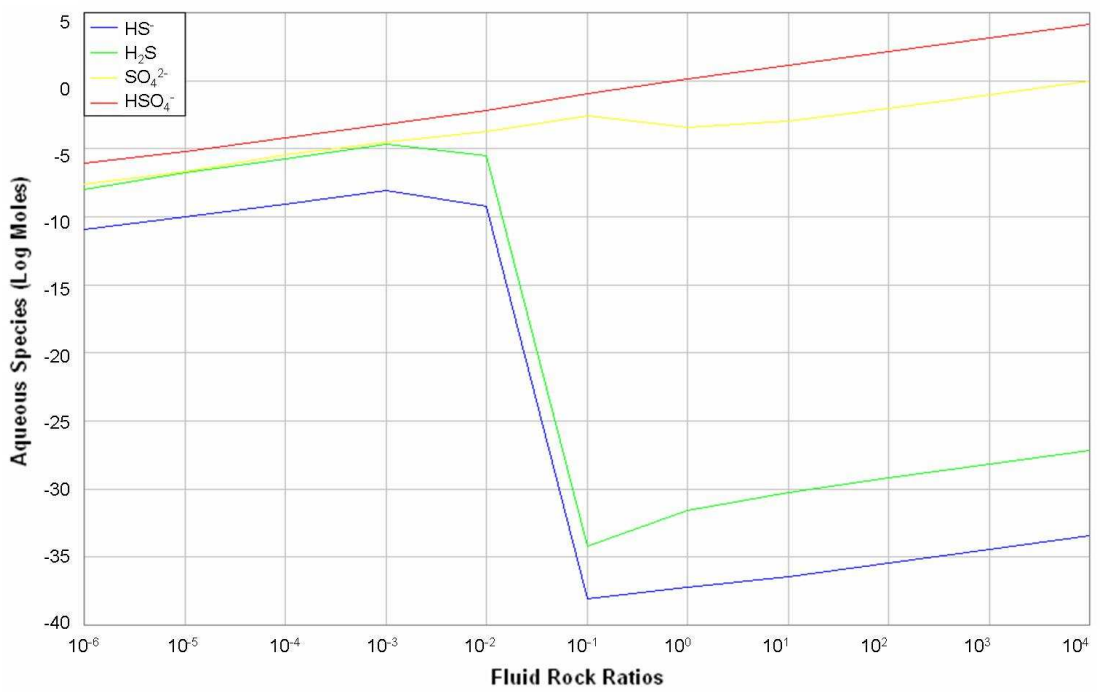

Figure 5.2: Dissolved sulphur species in CB fluid during reaction with Western domain type rocks at 600°C and 3000 bars.
At low fluid: rock ratios the host rock assemblage does not reduce sulphate species to sulphide with H_2S subordinate to SO_4^{2-} and sulphate remains dominant even at high fluid rock ratios

.

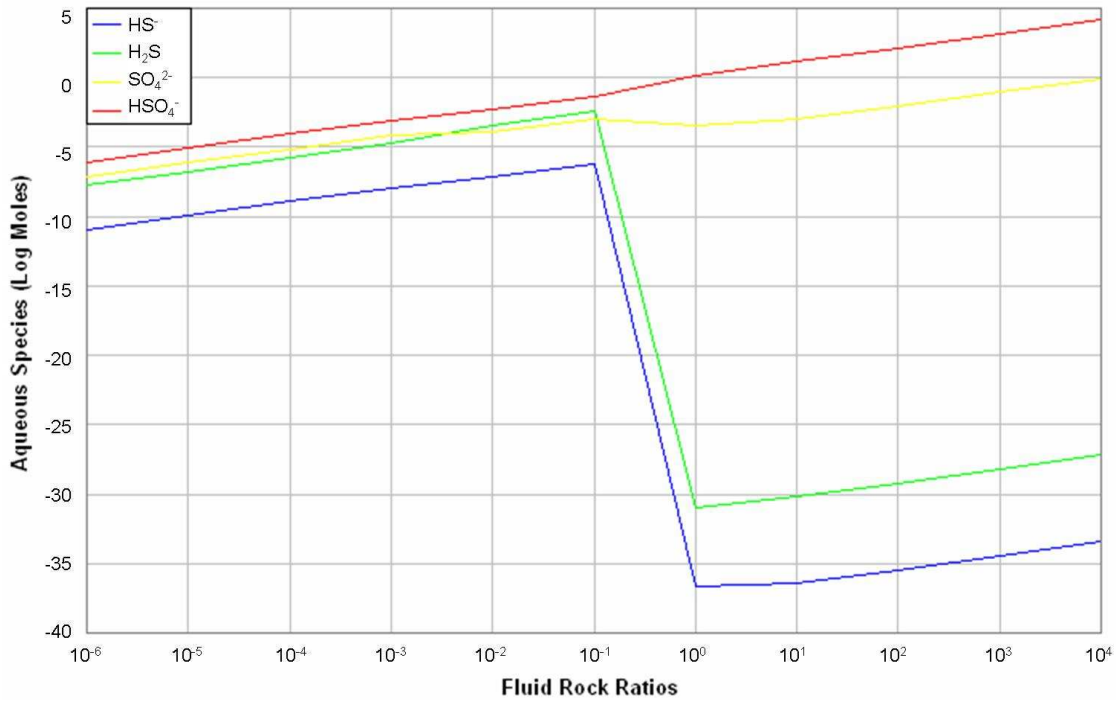

Figure 5.3: Dissolved sulphur species in CB fluid during reaction with Eastern domain type rocks at 600°C and 3000 bars
At low fluid: rock ratios the host rock assemblage does not reduce sulphate species to sulphide with H_2S subordinate to SO_4^{2-} and sulphate remains dominant at high fluid rock ratios, as observed in the Western domain (Fig. 5.2).

would limit the amount of SO_4^{2-} that could be dissolved in the fluid in a single fluid model.

The model results presented in figures 5.2 and 5.3 are for single fluid models assuming isothermal (600^{o}C) and isobaric (3000 bars) conditions. The fluid inclusion assemblage at Osborne documents cooling over the evolution of the deposit with secondary LVD inclusions indicating a decrease in temperature of several hundred degrees from peak temperatures of between 600 to 700^{o}C. Thus, cooling of the single fluid models must also be investigated (Fig. 5.4A; 5.4B). At low fluid rock ratios (Fig. 5.4A) the reduction of sulphate to sulphide is accomplished at low temperatures – due to the lesser buffering of the fluid oxidation state at lower fluid:rock ratios. However, this effect is not observed for steps with higher fluid:rock ratios (Fig. 5.4B) which can be considered more realistic of conditions at Osborne (Chapter 4).

5.3.3 Fluid Mixing Models

5.3.3.1 Flow-through models

The single-step batch process models described above have been tested for a variety of fluid:rock ratios. However, the maximum possible fluid:rock ratio should be constrained by the maximum possible porosity, typically less than 10% by volume at depth in the crust (Heinrich et al., 1996). A flow through model needs to be tested to more accurately model the high fluid:rock ratios accumulated by progessive fluid flow through a specific volume of rock.

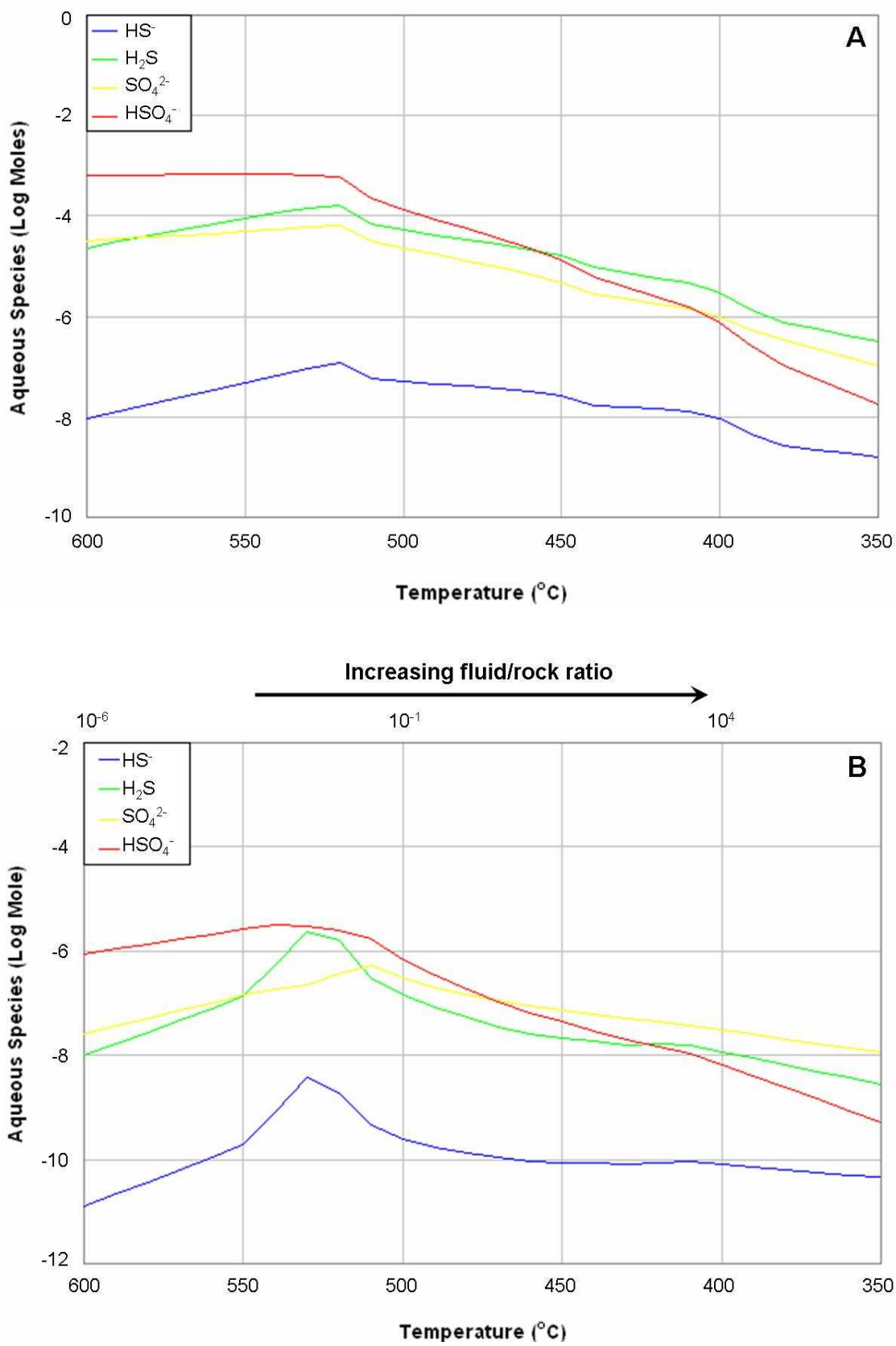

Figure 5.4: Cooling of CB fluid buffered by Western Domain rocks
(A) At a constant fluid:rock ratio of 10^{-3} dissolved sulphide becomes dominant species at lower temperatures.
(B) At higher fluid: rock ratios sulphate species remain dominant even at lower temperatures.

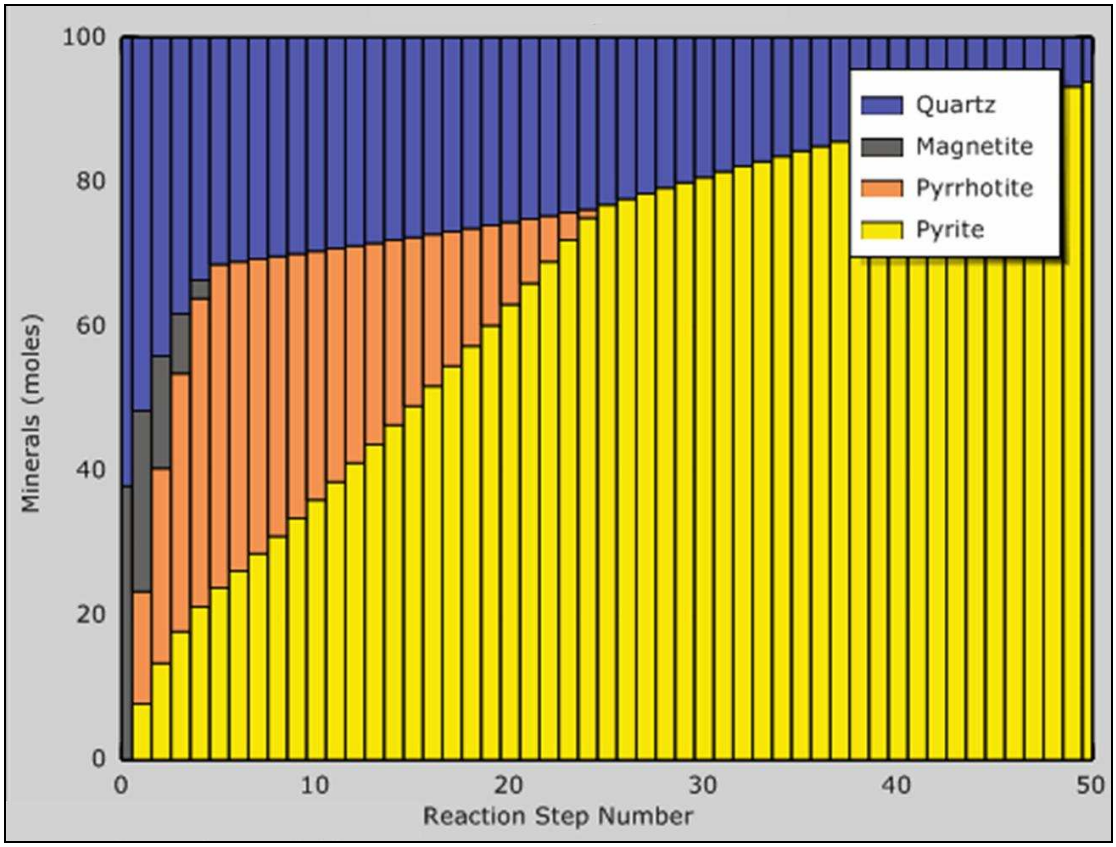

Figure 5.5: Flush model of ore fluids reacting with quartz-magnetite host rocks. Magnetite is consumed as sulphides are deposited.

The models presented in this section are simplified to examine the reaction of CB-type ore fluid with quartz-magnetite rock. This reaction is observed to have taken place in the Western domain where the sulphide mineralisation is associated with the banded ironstones (Chapter 2, Fig. 2.1A). In the first model a flush model is tested in which the chemical composition of the solid phase after reaction with the CB-type fluid in step 1 is passed on to step 2 and consequent steps in the reaction path. The model is run at 450^{o}C and 1500 bars which are at the lower end of the range of conditions calculated from microthemometric data for MS inclusions. Fluid mixing is modelled with sulphide transported by a second fluid, a low salinity brine with 2 moles of H_2S (a low salinity brine was chosen as a decrease in fluid salinity is measured over the course of ore formation at Osborne) and both fluids added to the quartz-magnetite rock simultaneously, with a fluid-rock ratio at each step of 1, cumulating to a fluid-rock ratio of 50 for the last step of the model. The results of this model are plotted as normalized stacked bars (Fig. 5.5), and show that as the reaction progresses the magnetite is consumed and quartz dissolved, with pyrrhotite and pyrite deposited. This is similar to processes documented by textures with the ore assemblage in which the sulphides are deposited in a second generation of quartz (Chapter 2, Fig. 2.5), but does not model the deposition of the second generation of quartz and at no point does chalcopyrite reach saturation so this model cannot be considered to truly represent ore deposition processes at Osborne.

5.3.3.2 Variable fluid mixing models

Having shown that a single fluid model is unlikely to have produced the Osborne ores, other precipitation mechanisms need to be considered. Halogen data (Cl:Br:I), which provides information on the source of ligands in the ore fluids, indicates

multiple sources of salinity (Chapter 3; 4) which has been interpreted as evidence for fluid mixing at Osborne. A fluid mixing model removes the importance of the host rocks as a reducing agent as reduced sulphur can be transported in a second fluid with mixing at the site of ore deposition implicated as triggering precipitation.

Studies of metal solubility in hydrothermal fluids suggest that Cu and Fe will be transported in chloride complexes while Au may be transported by either HS or Cl-complexes (see section 5.2). The variable Cu:Au observed at Osborne could be explained by mixing between two fluids, the first a Cu-bearing brine and the second fluid transporting Au and sulphur. Alternately the Au may be transported as a Cl complex in the brine and the variation of Cu:Au values is a function of changing redox state of the fluid during deposition. While PIXE studies of primary MS and CB fluid inclusions indicates the presence of sulphur in the brine fluid the concentration of sulphur can not be quantified (Chapter 4). However, as these fluid inclusions (at room temperature) do not contain chalcopyrite daughter minerals, which have observed in fluid inclusions in other Cu deposits (e.g. Mavrogenes and Bodnar, 1994), the reduced sulphur content of this fluid must be low. Modelling has shown that sulphate will not be reduced by reaction with the host-rocks at Osborne (Fig 5.2; 5.3). This is further evidence that a second fluid source is required to supply reduced sulphur for ore formation.

In these models an oxidised fluid end member is modelled as the CB-type fluid, which is predominately SO_4-bearing and equilibrated with pyrite and hematite. A second, reduced, end member fluid is modelled as a low salinity (1 molal) NaCl brine containing H_2S and CH_4 (Table 5.3). Mixing of an oxidised brine with a reduced ore

fluid has been invoked as a ore forming process for the Au-Cu-Bi iron oxide deposits of the Tennant Creek Inlier (Skirrow and Walshe, 2002). During mixing the redox balance is constrained by HSO_4:H_2S and H_2CO_3:CH_4 levels. Various fluid mixing scenarios were modelled in the presence of rocks with a western domain composition (0.37 kg quartz + 0.19 kg magnetite + 0.44 kg albite) and with variable fluid:fluid and fluid:rock ratios.

	[1] Eastern Domain rock	**[2] CB fluid**	**[3] Mixing fluid**
H_20	0	1.0 kg	1.0 kg
NaCl	0	2.3 mol	1.0 mol
KCl	0	9.2×10^{-1} mol	1.0×10^{-1} mol
$CaCl_2$	0	4.3×10^{-1} mol	9.0×10^{-1} mol
$FeCl_2$	0	1.3 mol	0
$MnCl_2$	0	1.0×10^{-1} mol	0
CuCl	0	5.0×10^{-4} mol	0
$ZnCl_2$	0	1.1×10^{-3} mol	0
$PbCl_2$	0	1.0×10^{-3} mol	0
H_2CO_3	0	0.5 mol	0
CH_4	0	1.0×10^{-3} mol	0.56 mol
H_2S	0	0.5×10^{-1} mol	0.5 mol
HSO_4	0	1.0 mol	0.5×10^{-2} mol
SiO_2	0.37 kg	0	0.37 kg
Fe_3O_4	0.189 kg	0	0.089 kg
MnO	0.001 kg	0	0.001 kg
Pyrite	0	0.1 kg	0
Hematite	0	0.9 kg	0
Albite	0.44 kg	0	0.44 kg
Dolomite	0	0	0.1 kg

Table 5.3: Fluid and rock compositions used in rock-buffered fluid mixing models (algorithms for each model specified in Appendix G).

5.3.3.2 Ore Mineral Assemblages

Three models are tested with different mixing proportions and alternately fresh and altered rock compositions acting as a buffer (see Appendix G for specific algorithms).

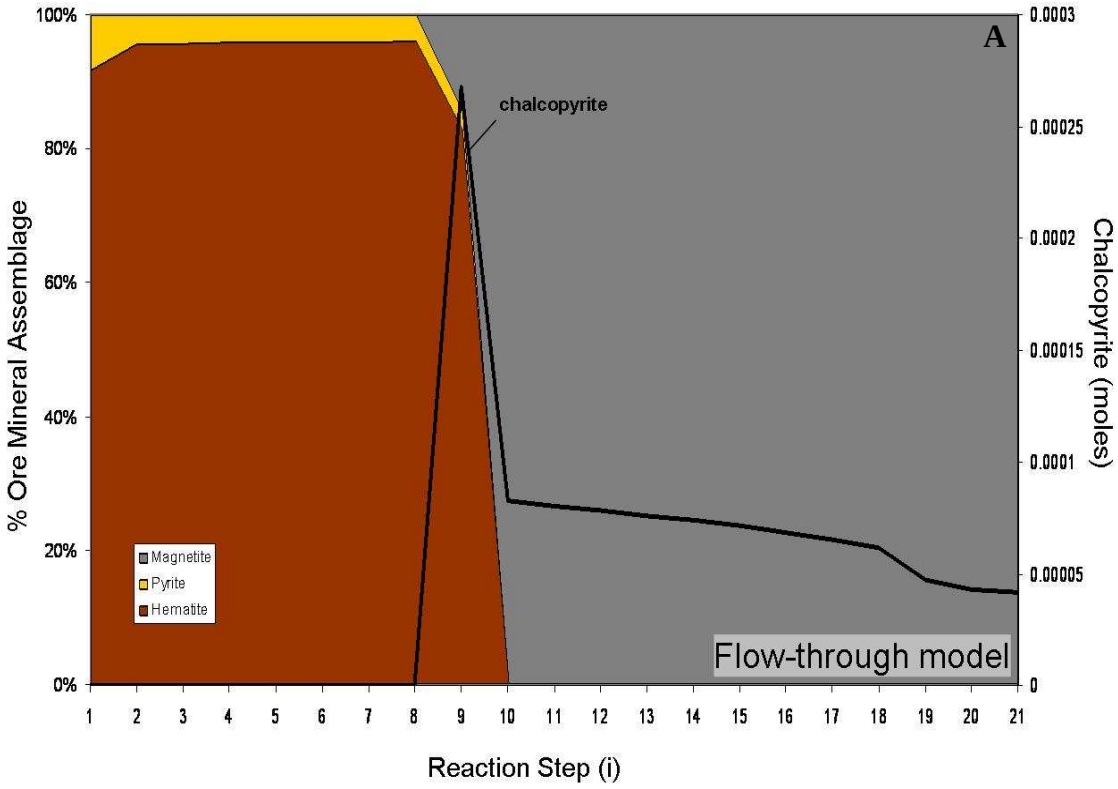

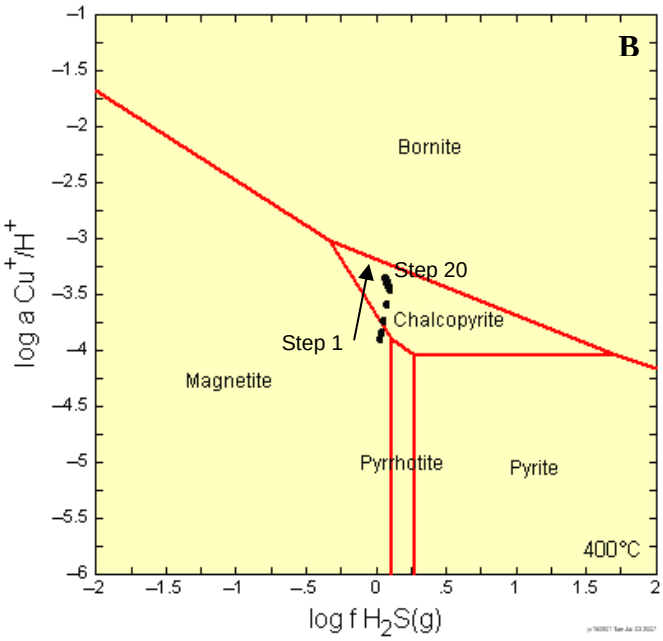

Figure 5.6: Fluid mixing and flow through model at 400°C and 2000 bars

(A) Chalcopyrite precipitation begins as the redox state of the fluid shifts from hematite-stable to magnetite-stable.

(B) Activity plot for log fO_2 = -25 at 400°C. As the reaction progresses the fluid moves into the field of chalcopyrite stability.

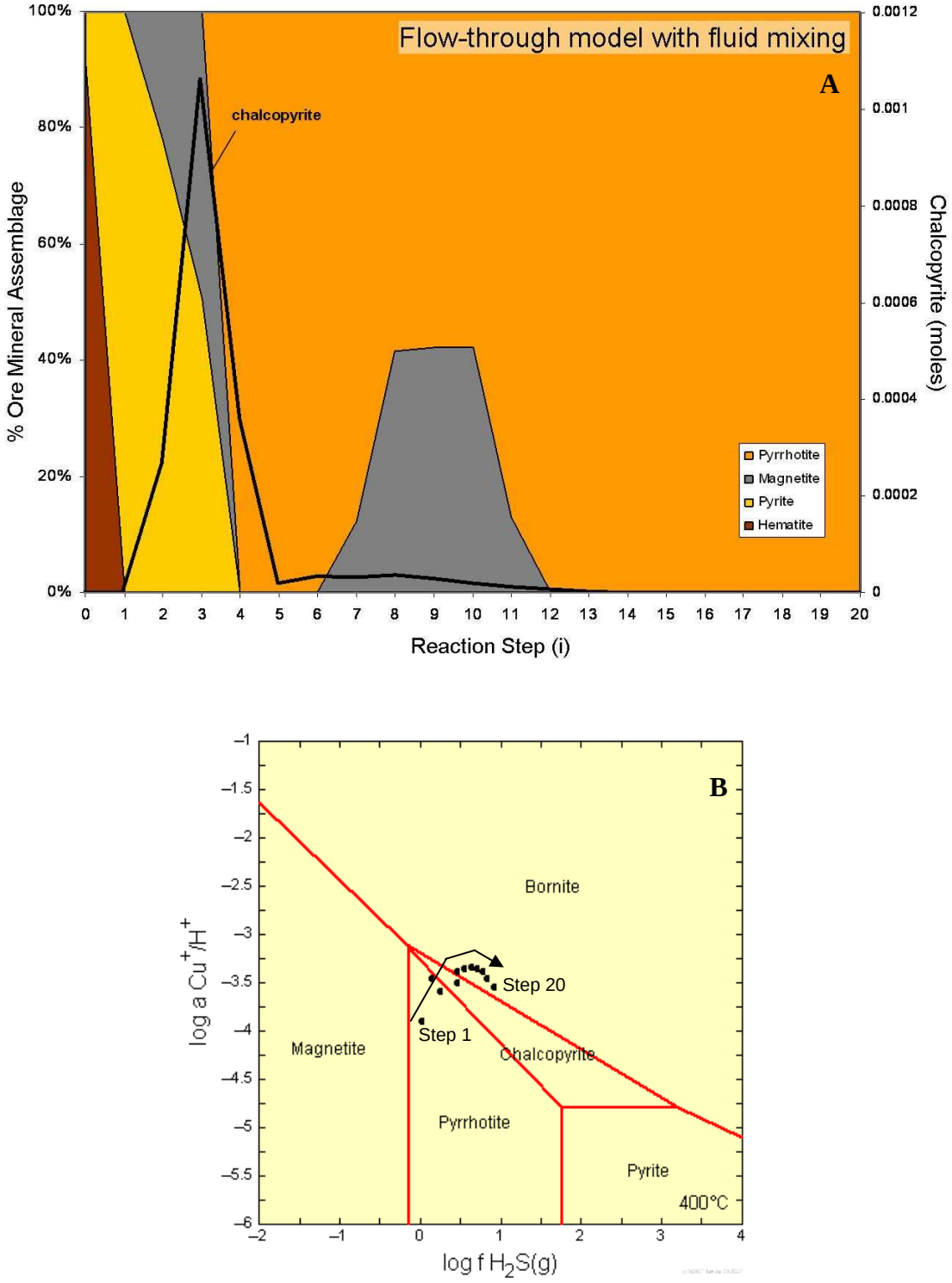

Figure 5.7: Fluid mixing model with additional titration of the reduced fluid phase at 400°C and 2000 bars.

(A) Chalcopyrite precipitation again is associated with a shift in redox conditions to magnetite and pyrrhotite stability.

(B) The activity plot shows the fluid moves into the field of chalcopyrite saturation as the reaction progresses and the proportion of reduced fluid increases. The points plotting in the bornite field are due to the diagram being plotted for an average log fO_2 value (= -29) while fugacity actually varies throughout the reaction. Diagrams at other log fO_2 values are plotted in Figures 5.6 and 5.8.

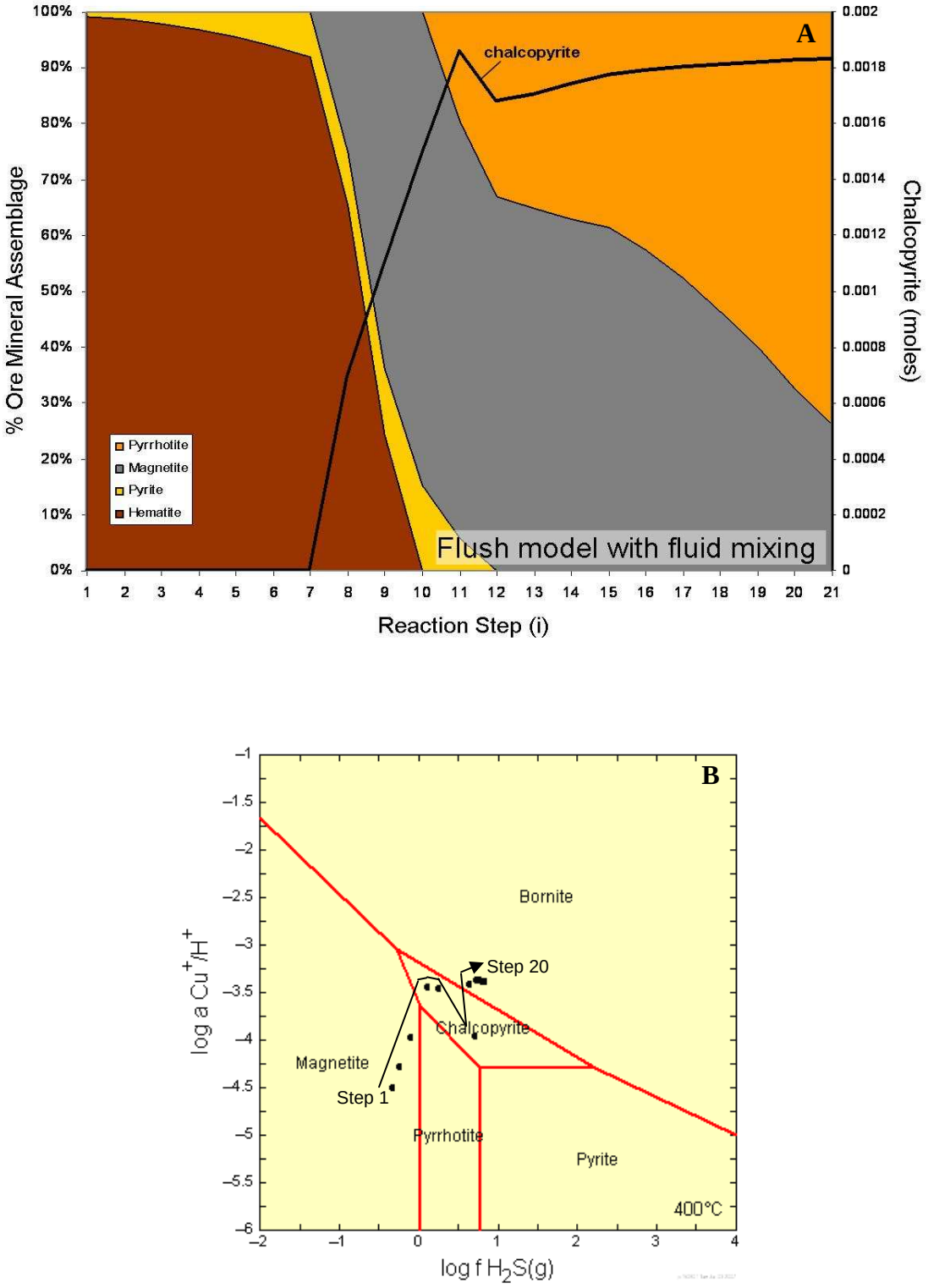

Figure 5.8: Fluid infiltration model with additional titration of reduced fluid at 400°C and 2000 bars.

(A) The peak in chalcopyrite precipitation is associated with a switch in redox conditions from hematite-pyrite to magnetite-pyrrhotite. Modelling suggests highest concentrations of copper ore will be associated with regions of with high fluid:rock ratios and where pyrrhotite forms part of the ore mineral assemblage. This correlates with relationships observed at Osborne.

(B) Again, the activity plots (log fO_2 = -26) shows that the system moves into the field of chalcopyrite stability as reduced fluid is added.

Firstly, a flow through model is tested; the two fluids are mixed in the first step and the reaction product moved through consecutive steps in the presence of Western domain rock at a fluid:rock ratio of 10:1 (Fig. 5.6). This fluid rock ratio was chosen as mass balance calculations indicate that there was high fluid flux during ore formation at Osborne (Chapter 4). In the second model the two fluids are mixed (step 1) and reacted with a western domain type rock (steps 2-20). The fluid phase composition is carried through each step and reacted with fresh rock with additional titration of the reduced fluid with each step (Fig. 5.7). In the third model the composition of both solid and fluid phase is carried through to the next step with additional titration of the reduced fluid in each step (Fig. 5.8). Modelling of similar scenarios but with the titration of additional oxidised fluid after the first stage of fluid mixing produces an oxidised hematite-pyrite assemblage in which there is no precipitation of chalcopyrite. In the models where the reduced fluid is added the chalcopyrite phase begins to precipitate as the redox state of the mineral assemblage shifts from oxidised (characterised by hematite + pyrite) to reduced (magnetite ± pyrrhotite). This suggests that the redox state of the fluids is an important control on chalcopyrite solubility at Osborne. Experimental and thermodynamic data on chalcopyrite solubility (see discussion in section 5.2) suggests that a shift from hematite-magnetite-pyrite stable conditions to magnetite-pyrite-pyrrhotite stable conditions will result in a decrease in Cu and chalcopyrite solubility (Seyfried and Ding, 1993; Liu and McPhail, 2005). The modelling results suggest that this redox shift was the trigger for ore deposition at Osborne. The importance of redox for deposition at Osborne may be enhanced due to the low concentrations of Cu in the Osborne ore fluids, which would have lessened the impact of temperature changes. Although it must be noted that the fluids modelled are a dilute proxy of the true ore

fluids which limits the extrapolation of the modelling results to the natural system. However, the variation in Cu:Au ratios observed at Osborne and its association with a redox gradient indicated by variations in sulphide mineralogy do support the important of redox controls on mineralisation at Osborne. The total sulphur content ($\sum$S) of the system will also be important, but as modelling has shown that reduction of sulphur can not be achieved by fluid-rock reactions (Fig. 5.2; 5.3) the addition of a reduced, sulphide-bearing fluid phase and resultant shift in redox state of the system can be considered important in triggering ore formation.

The models suggest that highest concentrations of chalcopyrite will be associated with regions that have seen highest fluid flux (i.e. Fig. 5.8 where fluid is added in each step to a solid phase which carries the composition forward through each reaction step, so that the each subsequent step has seen a greater fluid flux) and where the ore assemblage is most reduced. This correlates with observed mineralogy; the highest grade ore at Osborne is associated with pyrrhotite-rich zones within the ore bodies. This modelling emphasizes the probability of a reduced fluid component being involved in Osborne ore deposition.

The reaction paths for models 1, 2 and 3 are plotted on to activity diagrams (Fig. 5.6B; 5.7B; 5.8B) produced in Geochemists Workbench. The diagrams are created for conditions at 400^{o}C and 2000 bars, the same as the HCh models. The standard thermodynamic database used in Geochemists Workbench is restricted to temperatures below 300^{o}C and so to examine processes above this an alternate thermodynamic data file must be generated. For this study the UT2K utility was used to generate a log K file from the UNITHERM database, which is then converted for use

in Geochemists Workbench using the K2GWB utility as described by Cleverley and Bastrakov (2005). The log fO_2 for each model is calculated to produce diagrams specific to each model, although this value varies over the course of the reactions and only an average value could be calculated.

In each of the models described galena ± sphalerite is also precipitated. Precipitation of these phases commences after the peak of chalcopyrite saturation in all cases (e.g. Fig. 5.9). Modelling the same reaction process at 450^{o}C slightly suppresses the amount of galena precipitated, but has a greater effect on chalcopyrite (Fig. 5.9). As both Pb and Zn are measured in the pre- and post-deposition ore fluids at Osborne at the 100-1000's ppm level the absence of galena and sphalerite from the ore mineral assemblage suggests that conditions during ore formation must have remained very stable and have promoted chalcopyrite precipitation, to the exclusion of sphalerite and galena. In the model shown in figures 5.8 and 5.9 the onset of galena precipitation (at both 400^{o}C and 450^{o}C) is coincident with the start of pyrrhotite precipitation. This association indicates that redox may be an important control on the sulphide assemblage and the buffering of the fluids by the quartz-magnetite ironstones and albitised feldspathic psammites may be significant in maintaining the redox 'window' in which chalcopyrite precipitates leaving galena and sphalerite in solution. Examining the oxygen fugacity of the system as each phase begins to precipitate suggests that as the system becomes more reduced galena and sphalerite will precipitate (Fig. 5.10).

.

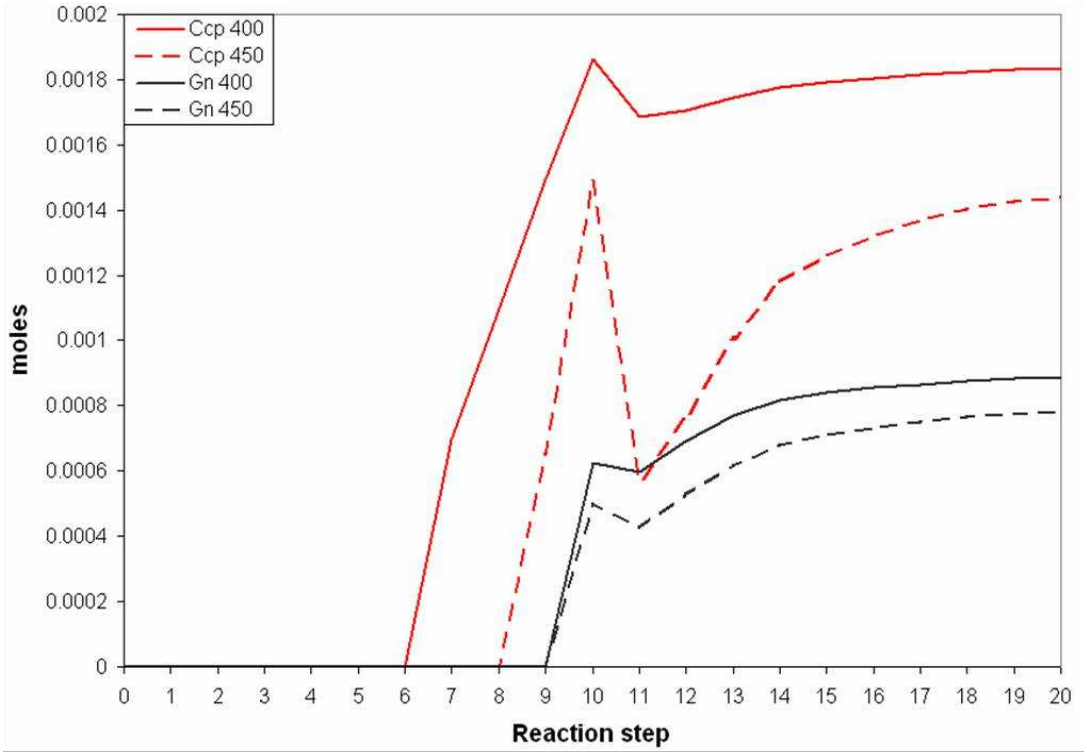

Figure 5.9: Chalcopyrite (Ccp) and galena (Gn) precipitation curves for model 3 (Fig. 5.8) at 400 ^{o}C and 450 ^{o}C.
The increased temperature has greater effect on chalcopyrite precipitation, with the start of chalcopyrite deposition delayed, whereas similar amounts of galena are deposited at both temperatures and precipitation begins at the same reaction step.

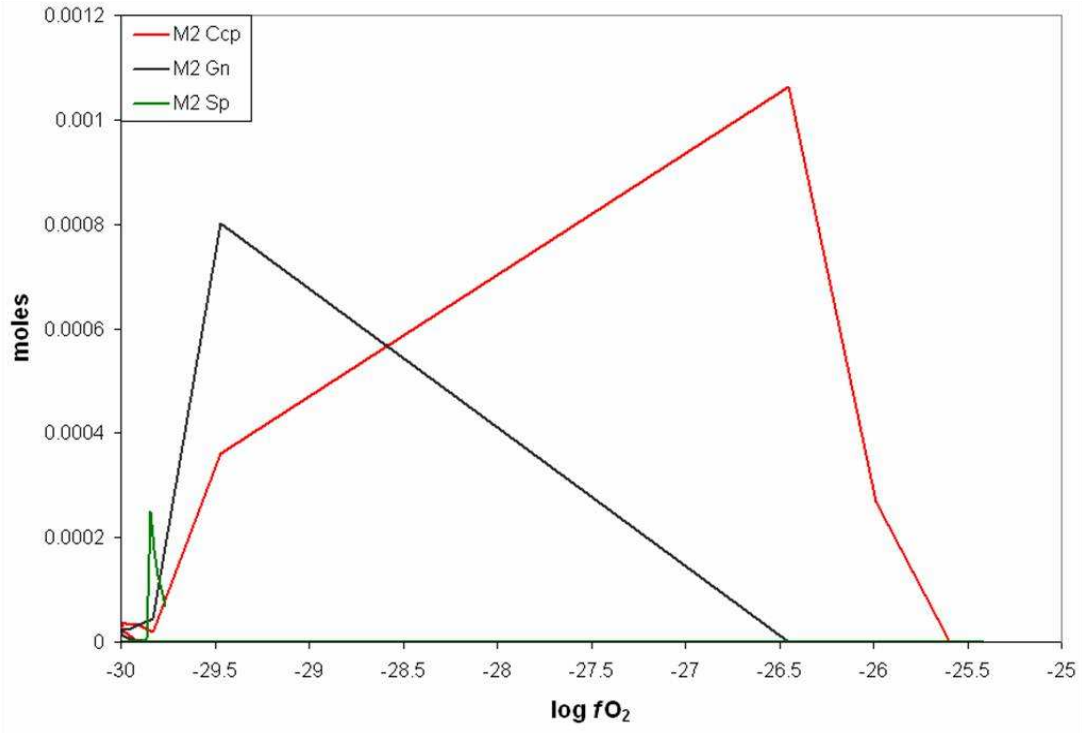

Figure 5.10: Oxygen fugacity vs. sulphide mineral yield for model 2 (Fig. 5.7).

The system becomes progressively more reduced as the reaction progresses. Chalcopyrite (Ccp) precipitates first and as log fO_2 values become more negative galena (Gn) and then sphalerite (Sp) are precipitated.

5.3.3.4 Alteration mineral assemblages

The main phase of Cu-Au mineralisation at Osborne is associated with the gangue silica-flooding. Associated wall-rock alteration assemblages include chlorite-talc-ferro-endenitic hornblende and talc-dolomite-hematite as well as biotite (Adshead, 1995). Adshead, (1995), identified a high temperature retrograde alteration assemblage that included actinolite, clinochlore and anthophyllite.

Alteration minerals produced during the simplified fluid mixing models described in this section include talc, clinochore, tremolite, ferro-tremolite, annite and phlogopite. Talc is an early phase in the models discussed (section 5.3.4.1) and with continued titration of reduced fluids disappears from the mineral assemblage. Biotite forms throughout the reaction and is dominated by the (Fe-rich) annite end member although the proportion of (Mg-rich) phlogopite present increases over the course of each reaction. The modelled alteration assemblage contains more Mg-bearing phases than are observed at Osborne. This is, in part, a function of having modelled the reduced fluid as in equilibrium with dolomite, in order to stabilize a lower fO_2 (dolomite can reasonably be assumed to be present in the region as part of the carbonate units of the Corella Formation). However, it may also be a result of not modelling amphibole and pyroxene phases as solid solutions in the way the biotite and plagioclase have been modelled, so that Fe-Mg fluid-mineral equilibria are improperly estimated.

5.4 Conclusions

Geochemical modelling of fluid processes at the Osborne deposit supports the conclusions drawn in earlier chapters:

- Fluid-rock reactions with sulphate bearing fluids will not result in reduction of the ore fluids and ore mineral precipitation.
- Cooling of a sulphate bearing fluid will result in sulphide precipitation in a single fluid model but only at low fluid rock ratios
- Reaction of the quartz-magnetite banded ironstones with the ore fluids will result in the destruction of magnetite and deposition of sulphides.
- Fluid inclusion studies suggest that sulphur was not transported in the CB-type brine.
- Therefore fluid mixing is preferred as an ore formation mechanism with the mixing of reduced and oxidised fluids causing precipitation of ore minerals and the sulphur transported in the reduced fluid, supported by the Ba content of the fluids.
- Modelling results suggest that dominance of the reduced fluid phase is required to reach significant deposition of chalcopyrite with deposition of copper associated with a redox switch.
- However, if the solid and fluid phases become too reduced, galena and sphalerite will become saturated.
- The absence of galena and sphalerite from the ore assemblage, despite the presence of Pb and Zn at the 100's to 1000's ppm level in the ore fluids, suggests that the redox conditions at Osborne remained fixed within a narrow range throughout ore formation, probably a result of rock-buffering.
- Redox must, therefore, be considered the dominant control on ore deposition during fluid mixing.
- The modelling results replicate the association of highest copper grades with the more reduced sulphide assemblages that has been documented at Osborne.

- The variable mixing between reduced and oxidised fluids to produce a spectrum of deposits with different redox states has been proposed as having produced the Tennant Creek Au-Cu-Bi IOCG deposits (Skirrow and Walshe, 2002). The fluid inclusion and modelling results at Osborne suggest a similar process may have occurred in the Cloncurry district and examples of a more oxidised deposit can be found at Starra (Rotherham, 1997a); where higher Cu concentrations in the ore fluids (Williams et al., 2001) would mean that more reducing conditions were not required for chalcopyrite deposition.
- However, development of a district-wide model for IOCG formation based upon findings at Osborne is complex given the earlier timing of ore formation at Osborne compared with other IOCG deposits in the region and would require a mechanism for the repeated tapping of fluid reservoirs to be identified.

6. CONCLUSIONS AND RECOMMENDATIONS

6.1 Key Findings on Osborne Ore Formation

- Hydrothermal processes at the Osborne IOCG deposit are documented by the fluid inclusion assemblage (Chapter 2). The main processes identified are:
    - Decompression resulting in the unmixing of a CO_2-bearing brine and precipitation of massive hydrothermal quartz.
    - Cooling and dilution of a high salinity brine over the period of Cu-Au ore deposition.
- Movement on deposit-bounding shear zones is suggested to be a probable cause of decompression, and the shear zones are identified as potential pathways for fluid flow (Chapter 2).
- Halogen data indicates multiple sources of salinity in the ore forming fluids (Chapter 3). Br/Cl and I/Cl data suggests that the end member compositions are:
    - A halite dissolution fluid
    - A bittern brine-like fluid
- The halite dissolution fluid end member has been identified as a fluid component in several Cu-Au deposits in the Cloncurry district including Eloise and Ernest Henry (Kendrick et al., 2006a; Kendrick et al., 2007).
- Noble gas data is compatible with sedimentary formation waters or locally derived metamorphic fluids being significant fluid sources at Osborne.
- The noble gas and halogen data is not consistent with an external magmatic fluid component such as that identified at Ernest Henry (Kendrick et al., 2007a). However, fluids derived from local anatectic pegmatites may be involved (considered magmato-metamorphic).

- The ore fluids have extremely high salinities with Fe and Mn contents equivalent to those measured in fluids of magmatic origin. The high metal and salt content of the fluids is attributed to the high temperatures and pressures the fluids reached (Chapter 4).
- The ore fluids have low Cu concentrations (<150 ppm) relative to other IOCG deposits in the Cloncurry district. At temperatures of 500-600^{o}C (as measured by microthermometry in MS-type inclusions) these fluids would have been significantly undersaturated with respect to chalcopyrite.
- Fluid mixing is identified as the most likely cause of Cu-Au precipitation with geochemical modelling suggesting that the resultant cooling and redox changes are the main controls on ore deposition (Chapter 5).

6.2 Key ingredients for an IOCG deposit

The study of ore forming processes at Osborne has identified key processes and fluid components that are important in ore deposition. However, the Osborne deposit formed over 50Ma before other known IOCG deposits in the Cloncurry district, making it less likely that it would share common fluid ingredients with the other deposits. Despite this, some common features can be established including the presence of a high salinity fluid that has interacted with evaporite sequences and the importance of fluid mixing as an ore deposition mechanism.

A magmatic fluid is not an essential component and has only been identified at one deposit in the region, Ernest Henry, using noble gas and halogen data (Kendrick et al., 2007a). However, Ernest Henry is the largest IOCG deposit in the Cloncurry district which raises the question of whether the presence of a magmatic fluid component is

required to form the largest deposits. Nd, O, H and S isotopic studies of IOCG systems in the Gawler Craton show a similar association. The highest grade and tonnage ore system in the region, Olympic Dam, has a primitive, mantle derived, fluid component while lower grade prospects do not record this fluid input (Skirrow et al., 2005). However, as the Osborne, Starra and Eloise deposits can not be considered low grade and have all been productive the data for the Cloncurry district suggests that fluid pathways that promote fluid mixing may be the more important criteria for ore formation.

The findings of this study and of studies of other deposits in the region (see Mark et al, 2004; Kendrick et al., 2006) suggest that IOCG deposits, even within a single district, can have both magmatic and non-magmatic fluid sources or a combination of the two. This is similar to findings in studies of IOCG deposits in South America (Chiaradia et al., 2006) which found that a spectrum of deposits were to be observed; from iron oxide-apatite and IOCG deposits associated with magmatic fluids to IOCG deposits associated with evaporitic fluids. That no single mechanism can be invoked to model the genesis of these deposits will be an important consideration when revising exploration strategies.

6.3 Recommendations for further work

- The comparison of PIXE and LA-ICP-MS data-sets suggests that using both methodologies in a single study can help to correctly measure elements that can be problematic for each method, particularly Ca. In this study the comparison was carried out using data on multi-phase and highly complex fluid inclusions. Further evaluation of the two methods using simpler inclusions with a well constrained fluid

chemistry would better allow the comparison of these two methodologies and identification of any systematic errors or differences between analyses using each method.

- Geochemical modelling of fluid-rock reactions could be used to provide exploration vectors. In particular modelling the reaction of pre- and post-ore deposition fluids and barren fluids with rock packages in the Cloncurry district and comparison of the results with actual alteration assemblages could help distinguish between prospective and barren alteration assemblages.
- The geochemical modelling at Osborne highlights the significant of redox as a control on ore deposition. The Starra deposit, situated to the north of Osborne, is associated with a more oxidised, hematite-rich, assemblage and ore forming fluids that contained concentrations of copper an order of magnitude greater than those at Osborne. Modelling of this system would offer a chance to study whether redox is consistently a dominant control on ore deposition in these systems.
- The noble gas and halogen data (detailed in Chapter 3) does not indicate a magmatic fluid component, and studies of other IOCG deposits in the region, including Starra, Eloise and Ernest Henry, have identified a magmatic component only at the Ernest Henry deposit. However, stable isotope studies at these deposits (i.e. Adshead, 1995; Baker, 1998; Rotherham et al., 1998; Mark et al., 2004) have indicated the involvement of a magmatic fluid component. Conducting a noble gas and halogen analysis of fluids exsolved from granites in the regions would establish whether fluids derived from the Williams and Naraku batholiths have halogen and noble gas compositions similar to those documented in porphyry copper systems of Phanerozoic age.

- Conducting stable isotope and combined noble gas and halogen data on samples from the same localities would help resolve fluid sources. $\delta^{34}S$ data would assist in assessing brine sources for the ore forming fluids.
- Finally He and Ne isotopes are also of use in studying fluid sources and can identify mantle-derived components in a fluid. While this analysis is outside the scope of this study, sulphide samples have been prepared for further noble gas analysis and the results will be presented in the future.